A THEORETICAL AND EXPERIMENTAL STUDY OF VIBRONIC INTERACTIONS IN THE RADICAL ANION SALTS OF TETRACYANOETHYLENE

By

JERALD JOHN HINKEL

Bachelor of science

Upper Iowa University

Fayette, Iowa

1970

Submitted to the Faculty of the Graduate College
of the Oklahoma State University
in partial fulfillment of the requirements
for the Degree of
DOCTOR OF PHILOSOPHY
July, 1974

A THEORETICAL AND EXPERIMENTAL STUDY OF VIBRONIC INTERACTIONS IN THE RADICAL ANION SALTS OF TETRACYANOETHYLENE

Thesis Approved:

Thesis Adviser

Dean of the Graduate College

ACKNOWLEDGEMENTS

I wish to express my sincere gratitude to Dr. J. Paul Devlin, research adviser, for the willing and patient guidance extended during this study. A special thanks is also due to Dr. Paul Westhaus for many valuable discussions.

My wife, Jeanie, and son, T. J., are most gratefully acknowledged for their encouragement, patience and sacrifices. Jeanie's patient and efficient preparation of this manuscript was greatly appreciated.

This study was supported by a National Defense Education Act Title IV Fellowship, the National Science Foundation, and the Oklahoma State University Chemistry Department. All financial assistance was greatly appreciated.

I would like to express my gratitude to Mr. Wayne Adkins and Mr. Heinz Hall for their competence and willing assistance when modifications or repairs were necessary.

Finally, I would like to acknowledge my fellow graduate students for their helpful discussions and comradeship.

TABLE OF CONTENTS

LIST OF TABLES

LIST OF TABLES (continued)

LIST OF FIGURES

CHAPTER I

INTRODUCTION

Tetracyanoethylene (TCNE) or, more systematically, ethenetetracarbonitrile, was first synthesized in 1957 by Cairns et al. (1) at du Pont. For purposes of illustration, the TCNE molecular geometry is diagrammed in Figure 1. Subsequent analysis of the reactions characteristic of TCNE established it to be an unusually strong π-acid. That TCNE should be a strong π-acid is supported by simple molecular orbital calculations (2) which indicate that the lowest unoccupied molecular orbital is only slightly antibonding. The abnormally high electron affinity of TCNE was established experimentally by Merrifield and Phillips (3). They observed that TCNE exhibits a strong tendency to form charge-transfer complexes. It was shown that TCNE would readily form weak complexes with xylene, mesitylene, etc. The diamagnetic properties of these complexes indicated that only partial electron transfer had taken place.

Later investigations (4) of the chemistry of the TCNE molecule showed that when TCNE is reacted with a species of suitably low ionization potential (e.g. alkali metals, Mg, Al, Zn, and Cu) complete electron transfer takes place yielding the TCNE radical anion. That the radical anion was, indeed, formed, was substantiated by electron paramagnetic resonance studies. The radical anion will be the focal point of the present experimental and spectroscopic investigation.

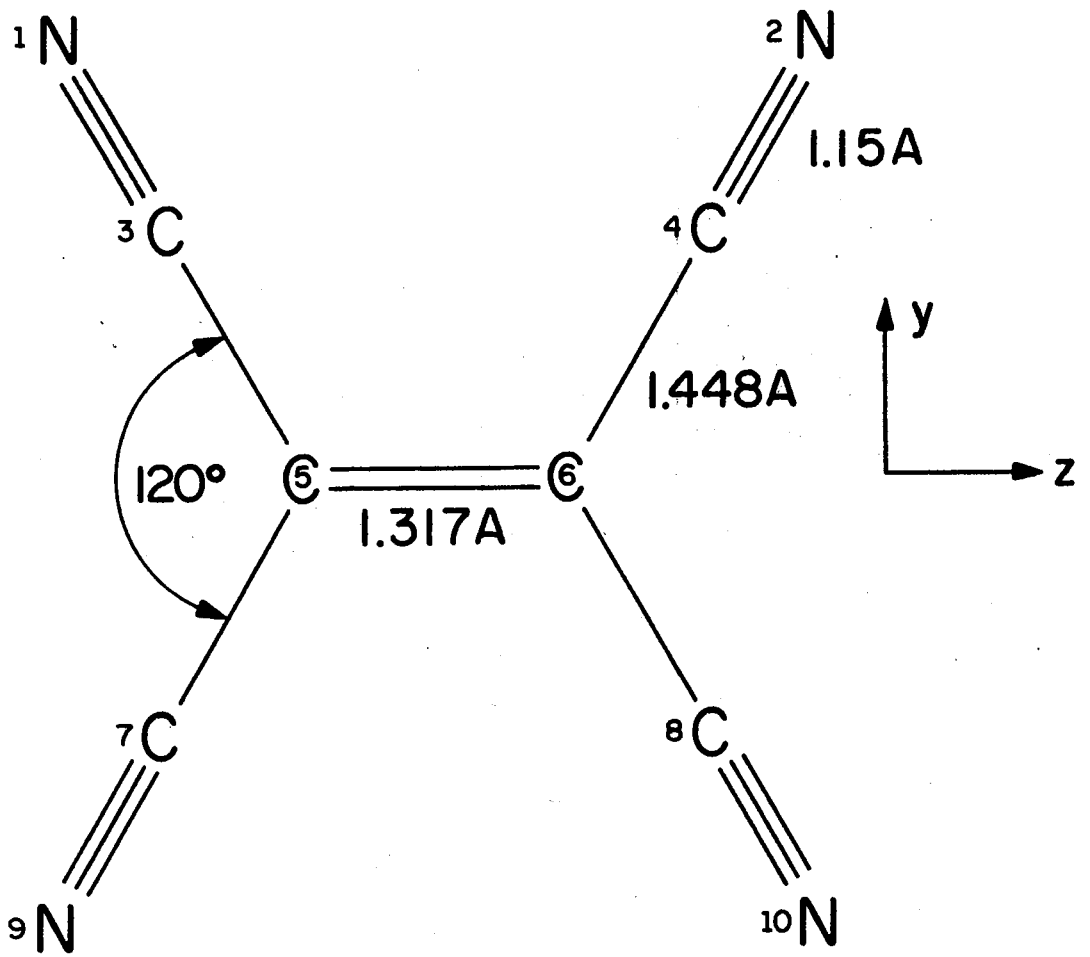

Figure 1. Structural Parameters for TCNE, all Bondlengths are in Angstroms. The atom-numbering scheme was used in the normal coordinate analyses and quantum chemical calculations

The infrared and Raman spectra of neutral TCNE has been studied quite thoroughly (5-8). Miller (6) et al. give a complete assignment of the vibrational modes. The subsequent normal coordinate analyses - performed as an aid for assigning the spectrum - show only fair agreement with the observed frequencies. Rosenberg and Devlin (8), using the overlay technique and a modified Urey-Bradley Force Field, were also unable to obtain a quantitative fit for ν_3 the totally symmetric (a_g of the D_{2h} molecular point group) carbon-carbon single bond stretching fundamental. Takenaka and Hayashi (5) also encountered difficulties in fitting ν_3. One of the aims of the present study is to correlate neutral and anionic force constants with the bond orders of the two species. For this correlation to be meaningful, a reliable set of force constants must be obtained. A normal coordinate analysis based on the Valence Force Field will also be undertaken.

The infrared spectra of thin film deposits of the radical anion salts of TCNE with various donors have been reported (9) (10). The infrared spectrum of the radical anion is remarkably different from that of the neutral molecule as may be seen from Figure 2. The only similarities between the spectra of the neutral and anionic molecules are the existence of far infrared bands which are assigned to out of plane modes and a doublet in the cyanide stretching region around 2200 cm^{-1}.

The infrared spectrum of the anion shows only extremely weak features in the 600-1350 cm^{-1} range which encompasses the frequencies where the carbon-carbon single bond modes (b_{1u} and b_{2u}) absorb strongly in the neutral molecule. Yet another striking discrepancy between the spectra is the intense absorption around 1370 cm^{-1} for the anion in a

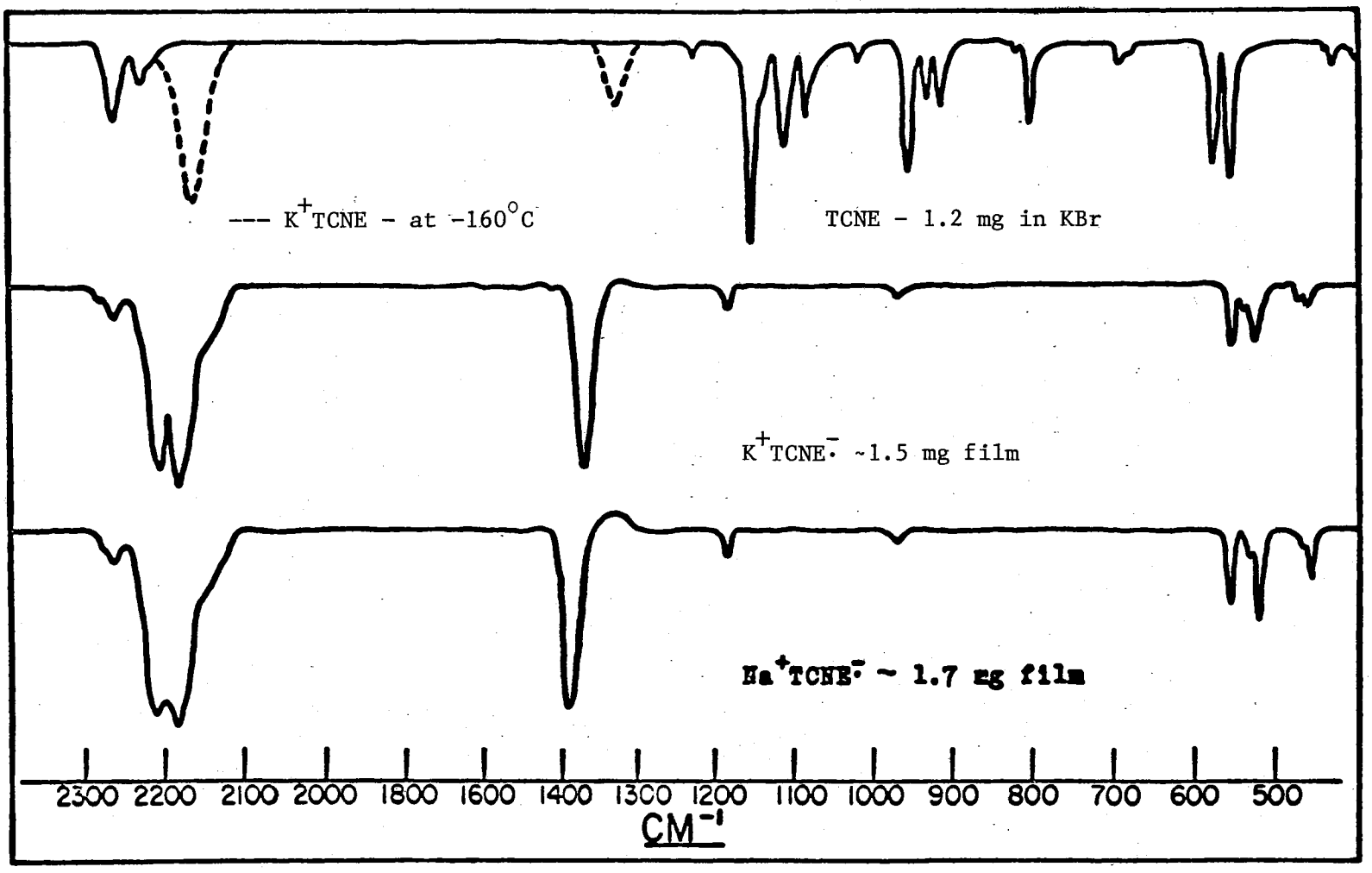

Figure 2. Infrared Spectra of TCNE and $TCNE^-$. These spectra were obtained from reference (9)

region barren of significant absorption in the neutral molecule. This intense band near 1370 cm^{-1} has been assigned to ν_2, the carbon-carbon double bond stretch, which is, of course, totally symmetric. Furthermore, all of the intense bands in the 600-2200 cm^{-1} region of the anion have been assigned to the totally symmetric stretching modes (9).

As mentioned earlier, neutral TCNE belongs to the D_{2h} molecular point group and, therefore, contains a center of symmetry. Invoking the mutual exclusion principle (11), one would predict that all normally active Raman modes (e.g. the symmetric modes) should be infrared inactive and vice versa. An obvious explanation of the unexpected anion result would be that neutral and anionic TCNE have radically different geometric structures and, hence, obey different vibrational selection rules. That this is the case may be ruled out on the basis of the work of Phillips et al. (4) in which it was shown that in the exchange reaction between the TCNE anion and tetracyanoquinodimethane (TCNQ) the anion is formed without severe structural modification.

Another explanation of the unusual differences between the spectra of the neutral and anionic molecules has been set forth (10). This explanation is based on the vibrational-electronic (vibronic) interaction mechanism. Assuming that the anion is located on an asymmetric site in the crystal, the stretching modes of a_g symmetry are presumed to be activated by an electron vibration (12) between the donor and acceptor species - in this case alkali metal and TCNE respectively. Further support of this assignment is given in the data of J. C. Moore et al. (10). They observed that as the ionization potential of the associated donor increases, the frequencies of the intense infrared bands in the anion spectrum approach the frequencies of the Raman bands

in the neutral spectrum. Furthermore, they observed that the directions of the frequency shifts - from neutral Raman to anionic infrared values - are entirely consistent with predicted bond order changes.

Other observations lend credence to the hypothesis that vibronic interaction effects play an important role in the infrared spectrum of the anion. First is the observation that conjugation of π-electrons has a pronounced effect on the intensities of certain infrared stretching frequencies (13). It has been fairly well established that vibronic interaction effects tend to occur most frequently in systems containing highly mobile electrons. The TCNE anion which is a conjugated system, with an additional mobile electron should, therefore, emerge a strong candidate when seeking a system with a reasonable probability of exhibiting vibronic effects.

Secondly, the theoretical interpretation of vibronic effects, which will be treated in detail in a later section of this chapter, requires that low-lying electronic excited states of the proper symmetry must exist. By proper symmetry, it is meant that the group theoretical reduction of the direct product of the irreducible representations of the excited state, ground state and the normal mode of interest must contain, at least once, the totally symmetric irreducible representation. When this condition is fulfilled, it is said that the particular excited electronic states may "mix" with the ground state during a vibration of appropriate symmetry. Actually no reduction is necessary here because all of the irreducible representations in the D_{2h} molecular point group are one-dimensional. In the TCNE anion, it should be recalled that the normal vibrations of b_{1u} and b_{2u} symmetries exhibit possible vibronic effects. Also along these lines is the fact that

certain out of plane modes in the far infrared region (200-600 cm^{-1}) retain their normal activity. This is entirely consistent with the vibronic selection rules since the ground and excited states have planar symmetry whereas the out of plane modes obviously do not. The preceding arguments are based on the vibronic selection rules derived by W. D. Jones (14).

From what has gone before, a reasonably strong argument can be made in favor of the utility of the vibronic interaction model in explaining the spectrum of the TCNE anion. The purpose of this investigation is to seek further insight, both experimental and theoretical, into the nature of vibronic effects in the TCNE radical anion.

Observation in the anion of reasonably intense Raman scattering at frequencies coincident with the intense infrared bands in the 600-2250 cm^{-1} region would verify that these intense infrared bands do, indeed, arise from totally symmetric modes. An earlier attempt (9) to monitor the Raman spectrum of the anion was thwarted by the intense color of the sample. In this study, an attempt will be made to prepare samples that will be spectroscopically suitable for both Raman and infrared measurements. The data obtained from these samples will then be used as a guide for the theoretical calculations. The theoretical problem is to estimate vibronic contributions to infrared intensities and to relate frequency changes (which should be equivalent to force constant changes) to changes in the bonding of the anion relative to the bonding in the neutral TCNE molecule.

Vibronic Interactions

A theoretical interpretation of vibronic transitions in polyatomic

molecules was first set forth by Herzberg and Teller (15) in 1933. The theory was devised to explain the appearance of certain weak, symmetry-forbidden electronic transitions in formaldehyde. The unavailability of suitable excited state wave functions prohibited any quantitative calculations of band intensities or oscillator strengths at that time. The theory proved to be qualitatively useful, however, in that it formulated a basis for vibronic selection rules. Their study was concerned with the effects that result when the nuclear coordinate dependence of the electronic wave functions is omitted. The approach was to treat the nuclear vibrations as perturbations on the equilibrium nuclear configuration electronic wave functions. This treatment makes the electronic wave functions dependent upon nuclear configuration. Their results indicated that certain electronic transitions that are forbidden in the zeroth order could become allowed through mixing of the zeroth order wave functions by certain non-totally symmetric nuclear vibrations. Development of molecular orbital theory and other approximate methods for dealing with many electron wave functions has made an extension of Herzberg and Teller's work possible.

Since the initial theoretical interpretation of vibronic effects in molecules was set forth by Herzberg and Teller (15), several more-quantitative papers have appeared in the literature. Craig (16), Murrel and Pople (17), Liehr (18) (19) and Donath (20) (21) have all attacked the forbidden intensity problem. Most of these papers (16-18) (20) (21) have dealt with symmetry forbidden electronic bands in the benzene spectrum. Pople and Sidman (22) have performed a theoretical intensity calculation on the $^1A_2 \leftarrow {}^1A_1$ (of C_{2v}) $n \rightarrow \pi$ transition of formaldehyde. Craig (16) utilizes the valence bond formalism whereas the other

aforementioned calculations are based on the molecular orbital theory.

The calculations by Murrel and Pople (17), Pople and Sidman (22), Liehr (18) (19) and Donath (20) (21) all follow the Herzberg-Teller (15) formalism. Albrecht (23) also utilized the Herzberg-Teller approach in developing a theory for calculating the forbidden character of allowed electronic transition intensities in para-disubstituted benzenes.

All of the aforementioned studies have been concerned with various ways of theoretically estimating both symmetry forbidden and allowed electronic transition intensities. This study is, however, concerned with the intensities of the pure vibrational transitions in the TCNE anion. The theoretical work on infrared intensities is quite limited. Several papers have undertaken a discussion of the infrared intensities of donor and/or acceptor bands in charge transfer complexes. Studies of band intensities in certain isolated molecules have also been reported. Before proceeding to examine the pertinent literature, it might be helpful to review the basic nature of the intensity problem itself.

The intensity of infrared absorption corresponding to excitation of the i^{th} normal mode is given by (24)

$$\Gamma_i = \frac{1}{nl}\int_{band} \ln \frac{I_o}{I}\, d\ln\nu = \frac{8\pi^3 N}{hc} P_i \qquad (1.1)$$

where the only undetermined quantity is P_i. P_i represents the probability of transition from the ground electronic, ground vibrational state to the ground electronic state with one quantum of excitation in the i^{th} normal mode, Q_i. The infrared transition probability is given by

$$P_i = [M_{go,gi}]^2 \qquad (1.2)$$

where $M_{go,gi}$ is a spectroscopically familiar term known as the

transition moment integral, or alternatively, the quantum-mechanical matrix element of the dipole moment, and is equal to

$$\int \bar{\psi}_{go}^{*} \bar{P}_{Op} \bar{\psi}_{gi} dqdQ = \int \phi_o^{*} \vec{P} \phi_i dQ \ . \tag{1.3}$$

The dipole moment operator, P_{op}, is given by

$$\bar{P}_{Op} = \sum_{i=1}^{n} -e\vec{r}_i + \sum_{\sigma=1}^{N} Z\sigma e\vec{R}\sigma \tag{1.4}$$

where n represents the number of electrons, N represents the number of nuclei and $\vec{r}_i$ and $\vec{R}_\sigma$ are the position vectors of the electrons and nuclei respectively. $\vec{P}$ is the dipole moment vector and is, of course, dependent upon nuclear coordinates. In Equations (1.2) and (1.3) above, the subscript g refers to the electronic ground state, whereas the subscript o and i represent the vibrational states of the molecule. The integration in Equation (1.3) extends over both the electronic coordinates q, and the nuclear coordinates, Q. The $\bar{\psi}$'s represent the total electronic-vibrational wave function (i.e. a product of an electronic wave function ψ with a vibrational function ϕ).

Equation (1.3) is often simplified by expanding the components of $\vec{P}$ in a Taylor's series with respect to the Q_i. The components of $\vec{P}$ are then just functions of the normal coordinates and integration over electronic coordinates is immediate. Invoking the harmonic oscillator approximation yields the following for the Cartesian coordinates, ξ and the n^{th} normal coordinate:

$$\int \phi_1^{*} P^{\xi} \phi_i dQ_n = \left(\frac{\partial P^{\xi}}{\partial Q_n}\right)_{Q_n=0} \int \phi_1^{*} Q_n \phi_i dQ_n = \left(\frac{h}{8\pi^2 c\bar{\nu}_n}\right)^{1/2} \left(\frac{\partial P^{\xi}}{\partial Q_n}\right)_{Q_n=0} \tag{1.5}$$

where the ϕ_j are the vibrational wave functions and $\bar{\nu}_n$ is the frequency

in cm^{-1} of the n^{th} normal mode. Substitution of this result into Equation (1.1) then yields

$$\Gamma_n = \frac{N\pi}{3c^2\bar{\nu}_n}\left(\frac{\partial \vec{P}}{\partial Q_n}\right)^2 \qquad (1.6)$$

where $\frac{\partial \vec{P}}{\partial Q_n}$ represents the change in the molecular dipole moment upon change of the n^{th} normal coordinate. Thus the infrared intensity may be seen to be proportional to the square of the dipole moment derivative. It is the dipole moment derivative that is usually sought in quantitative sutdies of infrared intensities. As can be seen from Equation (1.5), whenever the transition moment integral is zero by symmetry, the transition is said to be forbidden - this can be used as a basis for vibrational selection rules.

Coulson and Stephen (25) applied the molecular orbital theory to the ethylene and acetylene molecules. Their approach was to investigate how the electronic charge distribution varied during molecular deformation. The changes in the charge distributions were then used to estimate dipole moment derivatives and, hence, the infrared intensities of certain bending and stretching modes.

Ferguson and Matsen (26) applied Mulliken's (27) charge transfer theory in an attempt to explain the intensity enhancement of the symmetric ring stretching frequency of benzene in benzene-halogen charge transfer complexes. Their basic proposition was that intensity effects in charge transfer complexes result from a change in the amount of charge transferred from donor to acceptor during vibration. This change occurs because, in general, the potential curves of neutral and anionic species are not parallel. This theory predicts that the electron being transferred will oscillate between donor and acceptor

with a frequency equal to that of the fundamental that is enhanced. The electron vibration produces a rather large oscillating dipole moment and, hence, intense infrared bands. Using charge transfer theory, the authors were able to obtain a theoretical estimate of the dipole moment derivative for the benzene ring stretching mode.

Ferguson and Matsen later extended their studies to include the intensity of the stretching mode of the halogen component of the benzene-halogen complexes (28). An important aspect of the Ferguson-Matsen results was that infrared intensity enhancement of the halogen stretching mode could occur via the electron vibration mechanism even if the halogen molecule was in a "symmetrical" environment. Homonuclear, diatomic molecules have, of course, only one fundamental mode which exhibits Raman activity only. This result is very important in explaining the infrared spectrum of the TCNE anion.

Friedrich and Person (29) have noted that the effects observed by Ferguson and Matsen (26) (28) could be analyzed using a vibronic interaction type mechanism. Friedrich and Person (29) applied the work of Liehr (18) (19) to obtain an expression for intensity enhancement. Their derivation was considerably more rigorous than that presented earlier by Ferguson and Matsen (28), but would reduce to the earlier expression after the proper assumptions were made.

Treatment of vibronic interaction phenomena in isolated species has developed right along with the aforementioned studies of similar effects in charge transfer complexes. Most of this work has been done on the ever-popular benzene molecule (14) (16-21) (30) (32). Graham and Jones (33) studied the intensities of the fundamentals in the formate anion spectrum. Jones and Simpson (31) developed what was

subsequently termed the floating orbital theory and applied it to the model compounds H_3^+, H_5^+, and H_7^+. If the molecular wave function is made up by linear combination of atomic orbitals (LCAO), then the concept of floating orbitals can be described physically by specifying that the basis set atomic orbitals remain centered on the nuclei as they move. Thus, as the nuclei move, the electronic charge distribution changes.

Probably two of the best known investigations into vibronic effects on infrared intensities were developed by Jones (33) and Brown (30). The goal of both researchers was to estimate the extent of vibronic interactions in the benzene molecule. Brown (30) has developed an elegant theory based upon the earlier work of Liehr (18) (19), but using Pariser-Parr type wave functions (34) (35). The many assumptions that Brown (30) had to make in order to obtain a final numerical result may tend to invalidate his conclusion that vibronic interaction phenomena play an important role in the infrared spectrum of benzene. Jones (14), on the other hand, has derived a vibronic selection rule. This rule will be discussed in greater detail later, but it is interesting to note that Jones predicts vibronic effects in even-alternant systems to be quite small. Jones also presented some theoretical data based on both the molecular orbital and valence bond theories which indicate that reasonable results may be obtained via molecular orbital theory but not with the valence bond theory.

The theoretical foundation for the present study will now be laid. The goal is to obtain a theoretical expression for either the transition moment or the dipole moment derivative. Since the interest here is centered on the effect of the additional electron on infrared intensities in the TCNE radical anion, only the π-electronic or resonance

contribution to the transition moment will be considered in detail. The contributions due to the σ-electrons and nuclei is termed the framework contribution and will be assumed to remain unchanged in the neutral and anionic systems. An attempt will be made to estimate the framework contribution to the total transition moment. An increase in the absolute value of the sum of the resonance and framework contributions in anionic TCNE relative to that of the neutral can then be taken as reason to expect intensity enhancement of the particular fundamental being considered; similarly, a decrease in the magnitude of the sum should indicate intensity "washout".

The development of the theory of vibrational intensities to be presented here is quite similar to that presented by Hochstrasser (36) for the intensities of electronic transitions. Following Herzberg and Teller (15), the nuclear vibrations are treated as being perturbations that cause small variations in the total electronic energy as the nuclei execute small displacements from their equilibrium positions. The total electronic Hamiltonian is then expanded in a Taylor series with respect to the normal coordinates, Q_a. The perturbation is then taken to be the term in the expansion that is linear in Q_a. This result may be represented algebraically by

$$H' = \sum_{a=1}^{3N-6} \left(\frac{\partial H}{\partial Q_a}\right)_o Q_a \qquad (1.7)$$

where the partial derivatives in the expansion are evaluated at the equilibrium values of the normal modes, Q_a. The summation index runs from one to 3N-6, where N is the number of nuclei, because this is the number of vibrational degrees of freedom for a nonlinear, polyatomic molecule. The only terms in the electronic Hamiltonian that are

dependent upon the Q_a may be readily seen to be the nuclear-electronic attraction terms in the potential energy operator. In a later portion of this section it will be shown how H' can be obtained from a normal coordinate analysis of the molecule in question.

The nuclear coordinate dependence of the electronic wave function may be introduced via simple, first order, non-degenerate perturbation theory as

$$\psi_i^{(1)}(q,Q) = \psi_i^{(0)}(q,Q_o) - \sum_{j\neq i} \sum_a \frac{Q_a \langle \psi_j^{(0)}(q,Q_o) | \frac{\partial H}{\partial Q_a} | \psi_i^{(0)}(q,Q_o) \rangle}{(E_j^{(0)} - E_i^{(0)})} \psi_j^{(0)}(q,Q_o) \tag{1.8}$$

where $\psi_i^{(1)}(q,Q)$ represents a nuclear coordinate-dependent wave function that is correct to first order (indicated by the superscript) in the nuclear coordinate displacements. The $\psi_i^{(0)}$ are, as indicated in Equation (1.8), calculated for the equilibrium nuclear configuration.

It should be noted that non-degenerate perturbation theory should suffice for treating the TCNE anion problem, since the D_{2h} molecular point group contains no symmetry axes of order greater than two. A molecule must possess at least a C_3- axis as a symmetry element before any of the irreducible representations can have dimensions greater than unity - this is equivalent to saying that all representations in the D_{2h} point group are non-degenerate.

Equation (1.8) above shows how nuclear vibrations might mix or scramble the electronic states of the molecule. If any of the coefficients of the $\psi_j^{(0)}(q,Q_o)$ happen to be non-zero, then the first-order wave function will consist of a combination of the zeroth-order electronic wave functions.

As mentioned earlier, the quantity of interest for calculating

infrared intensities is the transition probability which is given by the square of the absolute value of the transition moment. Recalling Equation (1.3), the transition moment is shown to be

$$M_{ml,mi} = \langle \bar{\psi}_{ml} | \vec{P}_{op} | \bar{\psi}_{mi} \rangle \tag{1.9}$$

where, in the TCNE problem, $\vec{P}_{op}$ will represent only the π-electronic moment operator, and $\bar{\psi}_{mi}$ the vibronic wave function, is given as the product of a nuclear coordinate-dependent electronic wave function $\psi_m(q,Q)$ with a vibrational function ϕ_i^m which represents the i^{th} vibrational state of the m^{th} electronic state. Upon inspection of Equation (1.9), it may be seen that the electronic quantum number remains unchanged as is the case when treating vibrational transitions. For systems at or below room temperature, it can be safely assumed that the ground state electronic wave function is the appropriate choice. The vibronic wave function for the ground electronic, ground vibrational state can be formulated as

$$\bar{\psi}_{go} = [\psi_g^{(0)}(q,Q_o) - \sum_{j \neq g} \sum_a \frac{Q_a \langle \psi_j^{(0)}(q,Q_o) | \frac{\partial H}{\partial Q_a} | \psi_g^{(0)}(q,Q_o) \rangle}{(E_j^{(0)} - E_g^{(0)})} \psi_j^{(0)}(q,Q_o)] \phi_o^g(Q) \tag{1.10}$$

The transition moment for the transition from the ground electronic, ground vibrational state to the ground electronic state with one quantum of excitation in the i^{th} normal mode can be obtained by substituting the appropriate vibronic wave functions (e.g. ψ_{go} and ψ_{gi}) into Equation (1.9). After simplification, which includes properly accounting for orthogonality of and integration over the harmonic oscillator wave functions, the following result is obtained.

$$M_{go,gi} = -2\left(\frac{h}{8\pi^2 \bar{\nu}_i c}\right)^{\frac{1}{2}} \sum_{j \neq g} \langle \psi_g^{(0)} | \vec{P}_{op} | \psi_j^{(0)} \rangle \langle \psi_g^{(0)} | \frac{\partial H}{\partial Q_i} | \psi_j^{(0)} \rangle \left(E_j^{(0)} - E_g^{(0)}\right)^{-1}. \tag{1.11}$$

In Equation (1.11) above $\bar{\nu}_i$ is the frequency in cm^{-1} of the i^{th} normal mode, the $\psi_i^{(0)}$ are the zeroth-order electronic wave functions with energy $E_i^{(0)}$ constructed from either molecular orbital or valence bond methods, and $\vec{P}_{op}$ is the π-electronic moment operator.

How the perturbation integral may be obtained remains to be shown. This problem will be treated in detail in a later chapter. The perturbation integral can be evaluated only after a complete normal coordinate analysis of the system under consideration has been accomplished.

The quantity $(\frac{\partial H}{\partial Qa})_o$ has the symmetry properties in electron space as Q_a does in the nuclear space. This information is qualitatively useful in determining whether or not the integrals in Equation (1.11) will be non-zero on the basis of parity arguments. If one of the integrals happens to be zero, then vibronic contribution to the intensity would not be expected.

All that now remains to be done before infrared intensities can be calculated via Equation (1.11) is to choose some zeroth order electronic wave functions. The apparent success obtained using molecular orbital-type wave functions (14) (17) (20-22) along with its attendant simplicity will be taken as sufficient justification for adopting the molecular orbital formalism in this study.

Force Constant-Bond Order Changes

When the TCNE radical anion is formed, the additional electron goes

into a molecular orbital that is slightly antibonding (37). Due to the antibonding nature of the lowest unoccupied molecular orbital, the anion is predicted to be less stable than the neutral TCNE molecule. This instability is reflected in a decrease in the net bonding in the anion relative to that in the neutral molecule.

The TCNE molecule consists of a total of nine bonds, but due to the high degree of molecular symmetry there are only three different types of bonds: C-C, C=C, and C≡N. The addition of the antibonding electron must produce changes in the three bond types such that the overall effect leads to a less stable species. The changes in the bonding should be related to changes in the frequencies of the bond-stretching modes of anionic TCNE relative to those in the neutral molecule.

Bonding changes should also be related to bond order changes. The mobile π-bond order between atoms r and s as defined by Coulson (38) is given by

$$\rho_{rs} = \sum_{j=1}^{N} n_j c_{jr} c_{js} \qquad (1.12)$$

where n_j is the number of electrons in the j^{th} molecular orbital, c_{mn} is the coefficient of the n^{th} atomic orbital in the m^{th} molecular orbital, and N is the number of occupied molecular orbitals. ρ_{rs} is defined as zero if r and s are not neighboring atoms. Penfold and Lipscomb (37) have calculated bond orders for the neutral, mono-negative and di-negative TCNE species. Their results indicate that the multiple bonds suffer a decrease in bond order whereas the carbon-carbon single bond shows an increase in bond order. As mentioned earlier, this trend is consistent with the shifts of the neutral Raman bands to the infrared anion bands and was used as a supportive argument for assigning the

intense anion infrared bands to the totally symmetric stretches.

The bond order of a bond is generally taken as a measure of the strength of the bond. Bond order is quite often correlated with bond length (38-42), the idea being that a larger bond order (stronger bond) should result in a shorter bond and vice versa. If the bond order can be taken as a measure of the strength of a particular bond, then it should be directly related to the force constant for that bond. The bond order-force constant relationship has not been studied very thoroughly.

Badger (43) developed an empirical relationship that correlated the bond force constant with the bond length. This could be thought of as a bond order force constant correlation due to the bond order-bond length relationship. Unfortunately, Badger's (43) results were applicable to only a limited number of molecules.

Gordy (39) has also developed an empirical force constant relationship which seems to be at least intuitively reasonable in that it is based on quantities chemists often use to correlate bond strengths. Gordy's relationship is

$$k = 1.67N \frac{X_A X_B}{d^2}^{3/4} + .30 \qquad (1.13)$$

where k is the force constant for the bond joining atoms A and B, d is the bond length, N is the bond order, and X_A and X_B are the electronegativities of atoms A and B respectively. Gordy has applied this relationship to a number of molecules with reasonable success. It has been observed that molecules for which the valence force field is inadequate may not fit this rule. The valence force field will be used to calculate force constants for the neutral and anionic TCNE species

and these will then be compared to force constants calculated from Equation (1.13).

Eargle (49) has used the infrared frequency shifts of certain diarylketyl and TCNE radical anions to estimate electron spin densities. The reverse should also be possible, i.e. if the electron densities are known from either calculation (50) or the ESR spectrum (4), then it should be possible to predict frequency shifts. The concept of correlating electron spin densities with frequency shifts is analogous to that of relating frequency shifts to bond order changes, since both changes result from a change in the bonding.

Coulson and Longuet-Higgins (44) addressed themselves to the task of determining the changes in bond order that occur when Coulombic or resonance integrals vary. The variations occur during molecular vibrations because of the bond length dependence of the resonance integrals. They were able to obtain expressions for both diagonal valence force constants and off-diagonal interaction force constants. Their results led to

$$k_{rr} = \lambda_r + \frac{\mu\pi_{rr}}{\lambda_r^2} \tag{1.14}$$

and

$$k_{rs} = \frac{\mu\pi_{rs}}{\lambda_r\lambda_s} \tag{1.15}$$

where

$$\lambda_i = S(1-\rho_i) + k\rho_i \tag{1.16}$$

and

$$\mu = \tfrac{1}{2}k^2s^2(s-d)^2 \tag{1.17}$$

In the equations, s and d represent single and double carbon-carbon bond lengths respectively, k is the pure double bond force constant, ρ_i is the mobile π-bond order of the i^{th} bond, and π_{ij} represents the mutual bond polarizability of bonds i and j. The ρ_i and π_{ij} are functions of molecular orbital coefficients and energies which are obtained from the eigenvectors and eigenvalues of the secular determinant. Equations (1.14) - (1.17) have a much sounder theoretical basis than Gordy's (39) relation and have been applied quite successfully by Coulson and Longuet-Higgins (44). Gavin and Rice (45) have employed the Coulson result to estimate force constants for the linear polyenes and found it to yield reasonable results. Unfortunately, the Coulson-Longuet-Higgins result is not at present applicable to systems containing more than one hetero-atom. The appeal of being able to calculate force constants as readily as semi-empirical wave functions is great; therefore the possibility of modifying Coulson's argument to yield expressions valid for molecules with several hetero-atoms will be considered.

Jones (14), using vibronic interaction theory analogous to that developed in the previous section, has obtained the following expression for estimating the resonance force field:

$$f_i = \frac{\partial^2 V}{\partial s_i^2} \simeq 2\langle g|H_i'|e\rangle^2 \, (E_g - E_g)^{-1} \qquad (1.18)$$

In Equation (1.18) above, g represents the ground electronic state with energy E_g, e represents an appropriate (symmetry-wise) excited electronic state with energy E_e and H_i' is the perturbation operator as discussed in the previous section. It was found that Equation (1.18) yielded reasonable values for contributions to the vibronic potential

terms in benzene. These contributions result from mixing of the ground state with the E_{2g} and B_{2u} (of D_{6h}) electronic states upon deformation of the carbon skeleton.

In the present study, attempts will be made to correlate molecular force constant changes with bond order and energy changes. "Observed" force constants will be taken as those which best fit the observed vibrational frequencies. As mentioned earlier, a normal coordinate analysis will be undertaken utilizing a valence force potential function with necessary interaction constants. A comparison will then be made between these results and the earlier calculations that employed a Urey-Bradley-type potential function.

Resonance Raman Effects

The intense color of the TCNE radical anion salts together with the fact that the spectroscopic samples will be prepared in the form of thin films suggests the possibility that resonant Raman scattering might be observed. Resonant scattering from the symmetric skeletal mode of the anthracene dianion (highly colored, thin-film samples) has been observed (46). Since resonant Raman scattering is observed when the laser line used to excite the Raman spectrum aproaches an allowed electronic transition, the availability of several excitation frequencies greatly improves the chances of monitoring resonance effects. Also, the Raman intensity problem is theoretically similar to the problem of determining vibronic interaction effects; therefore, if vibronic interactions occur in the anion, then resonance effects might also.

CHAPTER II

EXPERIMENTAL PROCEDURES AND RESULTS

It has been pointed out earlier in this thesis that the infrared spectrum of the TCNE anion could be interpreted through consideration of vibronic interaction phenomena. In particular, the observance of an intense band near 1370 cm^{-1} concomitant with the "wash-out" of the bands in the 600-1300 cm^{-1} region can be explained in terms of vibronic interactions. Also, as was pointed out previously, all of the intense bands in the 600-2200 cm^{-1} range have been attributed to the a_g modes. The validity of this assignment would be strongly reinforced by observation of strong Raman bands at frequencies coincident, or at least nearly so, with the intense infrared absorptions. This chapter serves as a discussion of the experimental techniques involved in the preparation of samples of the TCNE anion suitable for Raman measurements. Following the discussion of the experimental procedures, a discussion of the data obtained will be undertaken with the aid of normal coordinate analyses. Finally, a discussion of the calculation of cartesian coordinate displacements will be given - the results of which will be used for calculating dipole moment derivatives in a later section.

Experimental Procedures

The alkali metal salts of TCNE have been prepared by co-condensation of the metal and TCNE onto substrates chosen to optimize the

infrared and Raman spectra. The techniques employed are simply an extension of those used in earlier infrared studies of the radical anion (9). A brief description of the experimental procedures and equipment used in this study is in order.

The vacuum cell used for sample preparation was a modified matrix isolation cell constructed by Smith (51). As mentioned earlier, the radical anion salts were prepared by deposition, under vacuum, of the TCNE and metal vapors onto spectroscopically suitable surfaces. The molecular and atomic beams originated from glass ovens which were surrounded by simple resistance heaters. The resistance heaters consisted of nichrome wire coils which had been calibrated by obtaining temperature versus voltage plots under experimental conditions. Optimum deposition temperatures and/or oven-orifice sizes were established by trial and error.

Re-sublimed TCNE and small freshly-cut pieces of the alkali metal, covered with n-heptane, are loaded into the ovens and evacuation of the cell is begun as quickly as possible. The temperature of the metal oven is raised to expedite the removal of the n-heptane coating. During this time, the infrared and Raman substrates are shielded to minimize contamination. After removal of the n-heptane, as indicated by the pressure in the system, the TCNE is raised to a temperature governed by the type of sample that is to be studied (e.g. TCNE-rich, metal-rich or a 1:1 ratio). The status of the deposition can be ascertained by observation of sample formation on the shield protecting the cryotip which supports the infrared and Raman substrates. Once deposition onto the protecting shield is proceeding smoothly and the desired TCNE-metal ratio (usually 1:1) has been achieved, the cryotip is rotated 90° to

expose the infrared prism and the Raman wedge to the oven vapors.

Adequate sample thickness was usually attained in ~ ½ hour. Generally an excess of TCNE was used in the formation of the 1:1 complex. The excess TCNE was initially present to inhibit the formation of the dianion, and was later removed by pumping on the system for ~ 2 hours at 10^{-5} torr. The sample was then cooled to liquid nitrogen temperatures for measurement of the vibrational spectra. Glass phase samples were also prepared by cooling the deposition substrates to liquid nitrogen temperatures prior to the deposition of the metal and TCNE.

The samples were deposited on a NaCl prism for the infrared measurements, and on an Al wedge for the Raman data. The wedge and prism were both mounted on the cryotip as close together as possible to insure sample uniformity on the two surfaces. Before each run, the cell was completely dismantled and cleaned thoroughly. All optical windows and the spectroscopic substrates were thoroughly cleaned and polished. Only silicone grease was used in or near the cell.

The infrared data were obtained using a Beckman IR-7. Raman measurements were obtained by the single reflection technique using the Al wedge. Raman scattering was excited using a Coherent Radiation Model 52 argon laser as a source. The Raman signal was detected with a Jarrell-Ash 25-100 dual monochromator with Hamner photon counting accessories. Due to the intense color of the sample coupled with its thin film character, resonant scattering was expected, and, in fact, observed. The Model 52 offers several excitation wavelengths ranging from 5145A(green) to 4579A(purple). The availability of several excitation frequencies made the observation of resonant scattering possible. The intensities of all of the lines used are typical of the Model 52

and range from ~0.7W at 5145A and 4880A to ~0.1W at 4579A.

Experimental Results

A successful run yielded thin films which uniformly covered both the NaCl prism and the Al wedge. The best samples appeared as highly-colored, reddish-purple transparent films. The purple color is characteristic of the 1:1 deposition ratio.

Figures 3 and 4 show both the infrared and Raman spectra of KTCNE and NaTCNE respectively. A comparison of the infrared and Raman peak frequencies in the two figures shows that each intense Raman band in the 500-2200 cm^{-1} region is coincident, or, at least very nearly so, with one of the more intense infrared features. This result is not necessarily significant in the C≡N stretching region since four modes of different symmetries appear in this region. The key observations to be made from Figures 3 and 4 are, however, the perfect coincidences in the infrared and Raman spectra at 523 and 1370 cm^{-1}.

As mentioned earlier, extensive infrared data strongly support the assignment of the intense band at 1370 cm^{-1} to ν_2, the a_g C=C stretching mode (9) (10). In the absence of strong resonant scattering (see, for example, the spectrum labeled b in Figure 3), the dominant Raman band in the 600-2100 cm^{-1} range is coincident with the intense 1370 cm^{-1} infrared feature. The band at 1420 cm^{-1} which, in certain samples, attains an intensity orders of magnitude greater than the intensity of the 1370 cm^{-1} band cannot be ignored. The feature at 1420 cm^{-1} assumes resonant character when 4880A excitation is used. The conclusion drawn here is, however, that both the 1370 and 1420 cm^{-1} bands originate from ν_2 in the anion. The 50 cm^{-1} splitting of the two bands is thought to arise

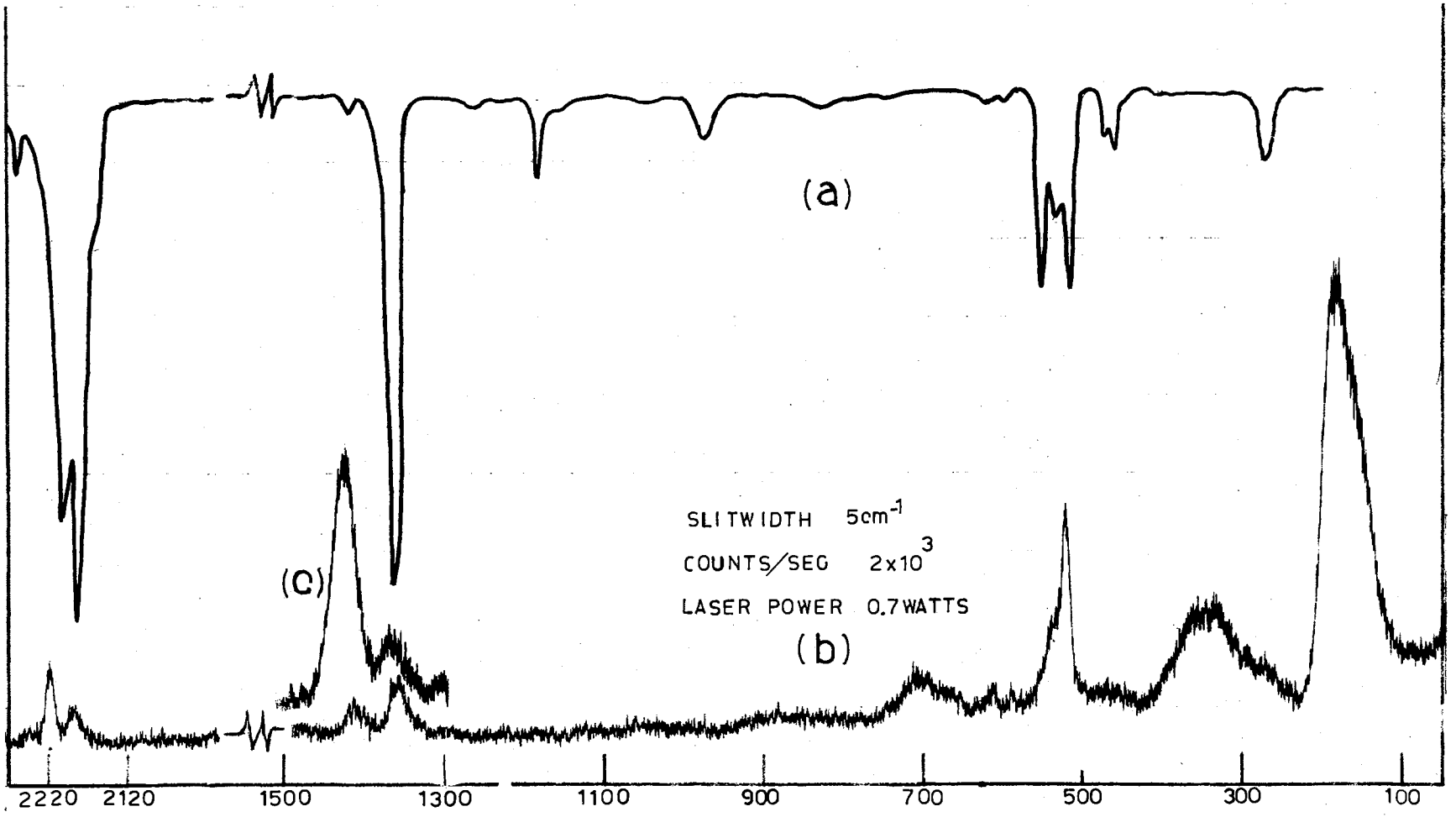

Figure 3. Vibrational Spectrum of KTCNE at -180°C: (a) infrared spectrum, (b) Raman spectrum with 5145Å excitation, and (c) Raman scattering with 4880Å excitation

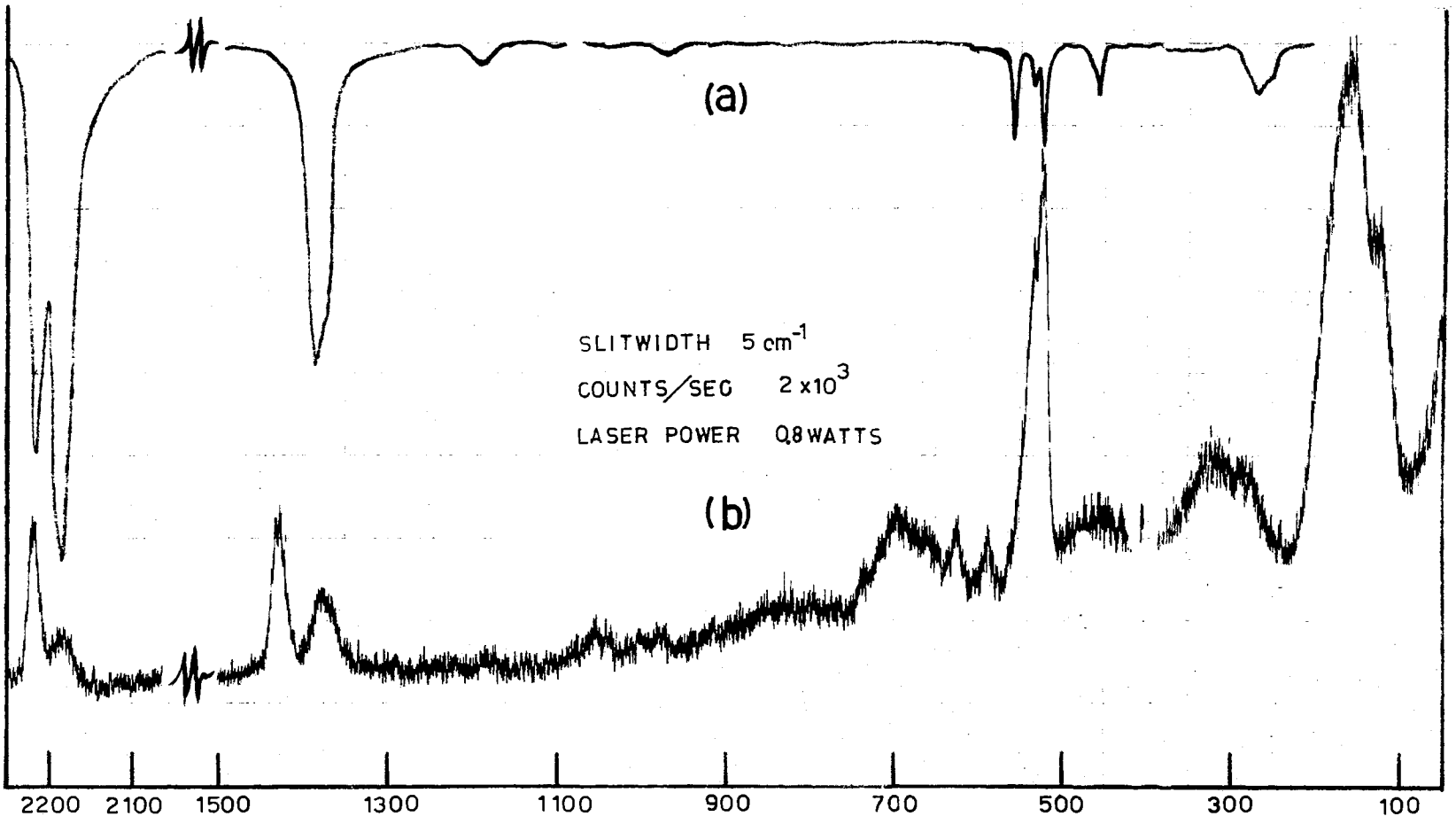

Figure 4. Vibrational Spectrum of NaTCNE at -180°C: (a) infrared spectrum and (b) Raman spectrum with 4880Å excitation. Note that the count rate is greater (5×10^3 counts/sec) below 400 cm^{-1} than at higher frequencies (2×10^3 counts/sec)

as a consequence of a dynamic coupling of either the factor group or transverse-longitudinal character. This assignment is strongly supported by a frequency increase of ~10 cm^{-1} in both bands when the metal counter-ion is changed from potassium to sodium - see Table I

The argument could be raised that, perhaps, neither of the bands at 1370 and 1420 cm^{-1} arise from ν_2. A consideration of the neutral TCNE spectrum shows only one other mode in this frequency range - the b_{3g} C-C stretch at 1280 cm^{-1}. Supposing that either the 1370 or 1420 cm^{-1} bands in the KTCNE spectrum arise from this mode, a consideration of cation electron affinities would lead to a predicted shift to a lower frequency in the NaTCNE spectrum. As may be seen from Table I, the opposite shift is observed.

A splitting similar to that observed in the bands at 1370 and 1420 cm^{-1} bands in the Raman spectrum is observed in the 2175 cm^{-1} band in the infrared spectrum. This splitting at 2175 cm^{-1} is attributed to crystal splitting since it is not observed in glassy deposits. A similar test for the 1370 and 1420 cm^{-1} bands in the Raman spectrum is not possible since the laser beam promotes crystallization of the glass phase samples.

As discussed earlier in Chapter I, the vibronic model also predicts that ν_3, the a_g C-C stretching mode, should produce strong Raman scattering at a frequency coincident with that of an intense infrared band. There are two moderately intense anion infrared bands in the 500-600 cm^{-1} range where ν_3 is expected to occur. In the absence of Raman data, these bands had been non-specifically assigned to an out-of-plane mode and ν_3 (9). As may be seen from Figure 3, the coincidence of the infrared band at 523 cm^{-1} with a strong Raman band allows a

TABLE I

INFRARED AND RAMAN BAND FREQUENCIES (cm^{-1}) FOR THE SODIUM AND POTASSIUM SALTS OF TCNE

KTCNE		NaTCNE		Assignment
IR	Raman	IR	Raman	
2196, 2175	2215, 2185	2222, 2188	2225, 2188	ν_1, C≡N sym. str.
	1960, 1900		----, 1910	$\nu_2 + \nu_3$
1420, 1370	1420, 1365	----	1430, 1380	ν_2, C=C sym. str.
		1385		
1187		1187		ν_{16}, b_{2u} C-C str.
			1050	$2\nu_3$
970		970		ν_{10}, b_{1u} C-C str.
	~700, 620, 590		~700, 630, 590	$4\nu_L$
553		556		ν_{23}, b_{3u} C-C≡N o.p. bend
537, 523	~540, 525	530, 521	~530, 523	ν_3, C-C sym. str.
470, 458		463, 455		ν_4, sym. C-C N bend
	~350, ~320, ~290		~350, ~320, ~290	$2\nu_L$
270		270		lattice mode?
	~175, ~160, ~140		~170, ~160, ~140	ν_L

specific assignment of ν_3 in the anion to be made.

The ν_3 mode in the neutral molecule has been assigned to a band at 679 cm^{-1} (5-8). The large shift (156 cm^{-1}) to a lower frequency by this band upon anion formation seemed unacceptable, particularly when bond order-force constant relationships would predict a shift in the opposite direction. This result, coupled with the failures of earlier workers to obtain satisfactory force constant-frequency fits to this value, led to a re-investigation of the solution spectrum of the neutral TCNE molecule.

TCNE was dissolved in methyl cyanide. The solution was placed in a conventional liquid-sample cell with the laser beam passed along the axis of the cell and the scattered radiation being measured at 90° to the beam path. Methyl cyanide has no interfering bands in the region of interest. Particular emphasis was placed on the depolarization ratios of the bands, since only the totally symmetric modes will be polarized. A polarized feature in the 500-700 cm^{-1} region is then taken to be due to ν_3.

The solution spectrum of the neutral TCNE in methyl cyanide is shown in Figure 5. The only polarized band of consequence is found at 535 cm^{-1} and is, therefore, assigned to ν_3. Further examination of Figure 5 shows that the 679 cm^{-1} feature is depolarized and, hence, the original vibrational assignments of the spectrum of the neutral molecule are in error. The 12 cm^{-1} shift observed for the anion (535-523 cm^{-1}) is more consistent with the shifts observed for other C-C modes. The anion infrared band at 553 cm^{-1} probably arises from an out-of-plane mode since a similar band appears at 554 cm^{-1} in neutral TCNE, and the intensities of bands for such modes are not

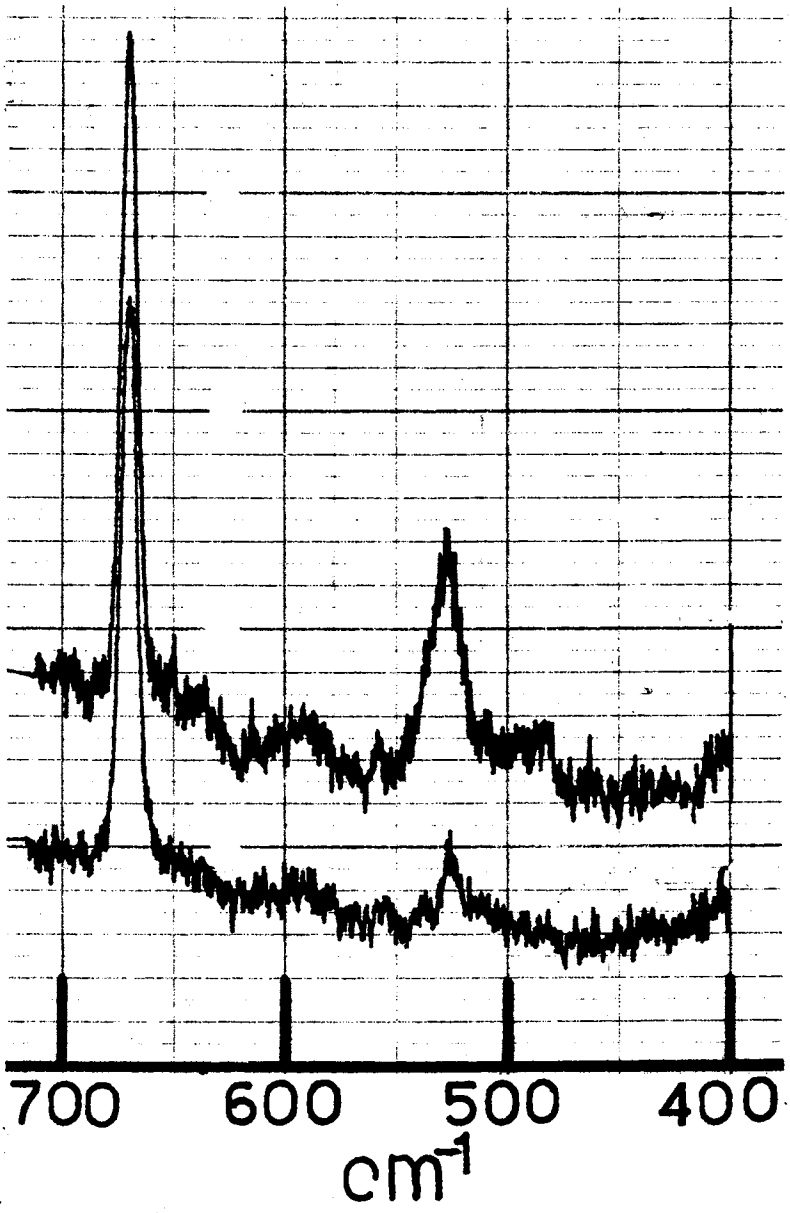

Figure 5. Raman Spectrum for Methyl Cyanide Solution of TCNE Showing Depolarized Character of the 679 cm^{-1} Band with Polarized Features at 490 cm^{-1} and 530 cm^{-1}

expected to be affected by a vibronic interaction.

Analogous to the other b_{1u} and b_{2u} in-plane modes, the TCNE planar bending modes are believed to have lost intensity due to vibronic interactions involving the radical electron. It is hoped that this observation can be put on a firmer basis by developing a theoretical model which would allow predictions of the π-electronic vibronic contributions to the intensities to be estimated. The model will be applied to the b_{1u} and b_{2u} C-C stretching modes.

Provided that the doublet band character near 2200 cm^{-1} results from a solid state splitting; only the ν_1 mode is required to explain the infrared and Raman features in this range. As mentioned previously, the argument that the doublet does, indeed, originate from a solid state splitting is reinforced by the sollapse of this splitting in the glass-phase samples. The lower frequency components of the doublet (~2188 cm^{-1}) are coincident within experimental error in the infrared and Raman spectra of NaTCNE and possibly KTCNE. The analogy of this doublet system with that of ν_2 also includes the effects produced by changing from green line to blue line excitation. In both cases, it is the higher-frequency component which is enhanced by resonant scattering. There is, however, a detectable difference between the infrared and Raman spectra in the peak position of the higher-frequency doublet component. This discrepancy is more apparent in the KTCNE samples as indicated by Figure 3. This result may be attributed to contributions from other C≡N stretching modes in addition to ν_1. It is thought, however, that the result is more probably due to a modification of the sample by local heating or photochemical effects. Two phases have been observed in the NaTCNE samples. The spectral shifts that

were observed between the two phases are approximately the same as the shift of the higher component of ν_1 in the infrared spectrum of KTCNE to the Raman spectrum.

Reference to Figures 3 and 4 shows a very intense, broad, low-frequency band near 175 cm^{-1}. The position of this band appears to be insensitive to the metal counter-ion used in the sample preparation. Inspection of fairly extensive experimental data does, however, show a dependence of the peak frequency of this feature on the precise deposition conditions, since it peaks anywhere in the range 150-180 cm^{-1} with the overtone bands responding accordingly. The band is thought to arise from a salt librational mode, ν_L.

Comparison of a large amount of data suggests that the ν_L band for a particular salt structure is sharp, but sample preparation procedures lead to the formation of several different crystal structures. A difference, from sample to sample, in which particular crystal structure is dominant explains why ν_L peaks out at a different frequency in different samples. Furthermore, since ν_L is sensitive to the particular crystal structure, and, since the actual sample is a composite of several structures, the observed band is expected to be broad - as is the case. In the $4\nu_L$ region, the individual features for the different structures are spread by a factor of four and appear as a weak series of bands from 590 to 710 cm^{-1}. The fact that bands resulting from internal modes are relatively sharp and appear at the same frequencies from sample to sample further supports the argument that ν_L must correspond to a composite of the lattice modes from different crystal structures.

The foregoing discussion of the experimental data fully supports earlier arguments as to the importance of vibronic phenomena in determining the vibrational spectrum of the TCNE anion. Also, an error in the earlier assignments of the spectrum of the neutral molecule has been noted. The information obtained will be used later in this chapter in normal coordinate calculations on the neutral and anionic molecules in an effort to obtain more meaningful force constant date for the two systems. Before proceeding to the normal coordinate analyses, however, a discussion of the resonant scattering observed will be undertaken.

Resonance Raman Effects

Resonant scattering effects assumed many forms throughout the Raman studies of the sodium and potassium salts of TCNE. Particularly interesting, was the observation that even those samples exhibiting almost identical infrared spectra would differ dramatically in their Raman spectra due to resonance effects. The resonance character of a particular sample seems, therefore, to be primarily a function of the sample character (i.e. crystal structure and stoichiometry). Due to the wide range of effects observed, no quantitative discussions can be presented. Certain trends and relative effects can, however, be discussed in a qualitative manner.

The band assigned to a librational mode, ν_L, near 175 cm^{-1} was invariably the most intense Raman feature for crystalline deposits regardless of the excitation frequency used (4579 to 5145Å). That a resonant scattering is associated with ν_L, is supported by the observation of overtone bands out to $5\nu_L$. It should be pointed out, though,

that the band corresponding to $3\nu_L$, which should appear at approximately the same frequency as ν_3, did not appear clearly in any of the spectra.

Normally, the internal mode band corresponding to ν_3 was the most intense internal mode band regardless of excitation frequency. But, as may be seen from Figure 4, in certain NaTCNE samples the higher component of the ν_2 doublet rivaled ν_3 in intensity when 4880A excitation was used. Furthermore, in one KTCNE sample, prepared at liquid nitrogen temperature, the band intensity near 1420 cm^{-1} was an order of magnitude greater than that for any other band.

The resonant character, in certain samples, of the ν_3 band is revealed when the scattering is excited using the 4579Å line; since, under these conditions, ν_3 appears only weakly. It appears that resonance effects also play a part in the ν_1 and ν_2 band systems. Excitation using either the 4579 or 4880Å laser line, rather than the 5145Å line, invariably produced an intensity enhancement in the higher-frequency components relative to the lower frequency ones.

Although resonant effects are important to some degree for ν_1, ν_2, and ν_3, the experimental evidence suggests that, of all the internal modes, ν_3 at 523 cm^{-1} participates most actively in the resonance Raman effects. That this should be the case is supported by the vibronic features exhibited in the electronic spectra of TCNE solutions (52). The solution spectra show vibronic fine structure with spacings of 540 cm^{-1} which correspond roughly to the frequency of ν_3. Several attempts were made to observe the vibrational structure on the electronic bands of the solid films prepared in this study. The attempts were unsuccessful, probably because, as the resonance character of ν_L suggests, the electronic bands of the solid films are composed of

numerous closely-spaced vibronic sub-bands which could not be resolved. These electronic spectra of the solid thin films did, however, show that the electronic band shifts into the 5000Å range, a necessary condition for the observation of resonance Raman scattering with the excitation frequencies used in this study.

The resonant character of the 1420 cm^{-1} component of ν_2 was observed to show extreme sensitivity to the precise sample character. A correlation between the degree of intensity enhancement of this band and the peak frequency of ν_L in NaTCNE samples has been deduced. It appears that a lower ν_L frequency leads to a greater enhancement of the ν_2 intensity when 4880Å radiation is used. Furthermore, it appears that the degree of resonance enhancement at 1420 cm^{-1} is a more sensitive indicator of sample character (crystal structures present, stoichiometry) than the positions of any of the infrared or Raman bands. The precise nature of this sensitivity was not ascertained.

Normal Coordinate Analyses

The reasons for performing normal coordinate analyses here are two-fold: 1) the earlier assignments given for neutral TCNE are in error, and 2) information regarding the anion stretching force constants relative to those in the neutral molecule is desired.

Several attempts have been made to fit the vibrational spectrum of neutral TCNE (5) (8). These earlier studies used the Urey-Bradley Force Field (UBFF) (5) and a UBFF modified by the introduction of resonance parameters (8). These endeavors led to a generally fair agreement between observed and calculated band frequencies. The most glaring discrepancy occurred in the inability to fit the strong Raman

band observed at 679 cm^{-1} which was then assigned to ν_3, the a_g C-C stretching mode. The result is now understandable in the light of the Raman solution spectra obtained in this study. As mentioned earlier, the depolarization ratios of the neutral molecule indicate that the band at 535 cm^{-1} should actually be assigned to ν_3.

A detailed discussion of the theory and equations used in normal coordinate analyses will not be presented here. A discussion of the calculation of cartesian displacement coordinates will be given later, however, since this is encountered less frequently.

A modified Valence Force Field (VFF) was used in the analyses presented in this study. Three bond stretching force constants (hereafter denoted $K_{C\equiv N}$, $K_{C=C}$, and K_{C-C}) along with three valence-angle-bending force constants ($H_{C-C=C}$, H_{C-C-C}, and $H_{C-C\equiv N}$) make up the constants appearing in the VFF. The VFF was modified through the incorporation of bond stretching interaction terms ($F_{C=C,C-C}$; $F_{C-C,C\equiv N}$). It should be explained that $F_{C-C,C\equiv N}$ and $F_{C-C,C=C}$ denote interactions only between adjacent bonds.

The calculations were carried out using the well known computer program, "Overend" (53). The bond lengths which are used in computing the G-matrix elements were taken from the crystallagraphic data given by Penfold and Lipscomb (2) and all bond angles were set at 120°. Due to the relative insensitivity of G-matrix elements to small changes in bond lengths, coupled with the lack of experimental data regarding anion bond lengths, the same G-matrix is used in both the neutral and anion calculations.

Thus, eight force constants must be fitted to the observed vibrational frequencies. Only 15 of the 17 planar vibrational frequencies

were used in obtaining the fit given in Table II. The band listed at 510 cm^{-1} was assigned by Takenaka and Hayashi (5) to ν_8, the b_{3g} C-C≡N bending mode. The Raman data obtained in this study show no evidence for this band and it was not, therefore, weighted in the least squares fitting procedure. Also, an infrared band at 119 cm^{-1}, which was at the detection limit in the earlier studies, was assigned zero-weight.

On the basis of the calculations done in this study, it was found that the bands assigned to the b_{1u} and b_{2u} C≡N stretching modes in the earlier studies should be interchanged; this has been done in Table II.

Inspection of Table II shows that the calculated vibrational frequencies agree very well with the observed values in all cases except at 510 and 119 cm^{-1}; but, as was previously stated, these values are uncertain and not weighted in the least squares fitting procedure. The average error of the calculated frequencies is only 1.7%.

The loss, in the anion, of the infrared activity of the b_{1u} and b_2u modes coupled with the failure to observe any Raman bands other than those resulting from lattice modes and internal modes of a_g symmetry makes a complete force constant analysis for the anion an impossibility. The problem is that there are only six observed anion vibrational frequencies, and, if an analysis similar to that done for the neutral is desired, eight force constants to be fit. This is clearly an under-determined case. Making the reasonable assumption that only the bond stretching force constants are appreciably affected upon anion formation reduces the problem to one of fitting three force constants with six frequencies. It should be pointed out that the average of the frequencies of the ν_1 and ν_2 doublets were taken as the "observed" frequencies in the anion.

TABLE II

OBSERVED AND CALCULATED PLANAR TCNE FREQUENCIES AND CORRESPONDING VALENCE FORCE FIELD FORCE CONSTANTS

	ν Obs. (cm^{-1})	ν Calc.	Assignment	Force Constants	
a_g	2235	2235	C≡N str.	K_{C-C}	5.32
	1569	1569	C=C str.	$K_{C=C}$	6.59
	535	558	C-C str.	$K_{C\equiv N}$	17.04
	490	489	C-C		
	130	133	(CN)-C-(CN) scissoring	$H_{C-C=C}$	0.43[b]
b_{3g}	2247	2257	C≡N str.	H_{C-C-C}	0.96
	1282	1287	C-C str.	$H_{C-C\equiv N}$	0.38
	(510)[a]	452	C-C≡N bend		
	254	245	(CN)-C-(CN) rocking	$F_{C=C,C-C}$	0.12
b_{1u}	2230	2231	C≡N str.	$F_{C-C,C\equiv N}$	-0.06
	958	953	C-C str.		
	579	558	C-C≡N bending		
	165	182	(CN)-C-(CN) scissoring		
b_{2u}	2263	2253	C≡N str.		
	1155	1152	C-C str.		
	443	440	C-C≡N bending		
	(119)[a]	81	(CN)-C-(CN) rocking		

a - Not weighted in this calculation. Our improved Raman data show no evidence of 510 cm^{-1} band and the 119 cm^{-1} IR feature was at the limit of the detectability in the original IR work.

b - Bending constants are in units of 10^{-11} ergs $radian^{-2}$.

The results obtained from the normal coordinate analysis of the anion are presented in Table III. Once again the agreement is seen to be quite good. The average error for the calculation was 1.23%.

It is felt that the two assignment changes discussed earlier for the neutral molecule and the ability to obtain good fittings of the observed frequencies for both the neutral and anionic molecules has led to the determination of reliable force constant values for both systems.

An interesting consequence of these calculations is the dramatic reduction predicted for $K_{C=C}$ in the anion relative to the value predicted for the neutral molecule. Simple bond order-force constant correlations would predict a reduction in $K_{C=C}$ upon anion formation, but the extent of the reduction seems surprising. Indeed, the anion results indicate the "double bond" to be weaker than the single bonds. It is hoped that the bond order-force constant relationship to be developed in the following chapter will offer some insight into this result.

Cartesian Displacements

Normal coordinate calculations are generally not carried out to the extent of computing the cartesian displacements of the nuclei. Probably the principal reason for this is the fact that normal mode forms can be ascertained by simply considering the changes in either internal or symmetry coordinates that occur during a normal vibration. This approach is sufficient if only symmetries or qualitative views are necessary. In this study, however, calculations of dipole moment derivatives are sought and, therefore, a detailed account of the nuclear

TABLE III

CALCULATED FREQUENCIES AND STRETCHING FORCE CONSTANTS FOR THE TCNE ANION

	ν Obs.[b]	ν Calc.	Assignment	Force Constants (md/A)	Observed[a]
a_g	2200	2201	C≡N		
	1392	1392	C=C	$K_{C\equiv N}$	16.34
	532	565	C-C		
	464	466		$K_{C=C}$	4.54
	---	132			
b_{3g}	---	2231	C≡N	K_{C-C}	5.68
	---	1308	C-C		
	---	454			
	---	246			
b_{1u}	---	2198	C≡N		
	970	967	C-C		
	---	563			
	---	181			
b_{2u}	---	2226	C≡N		
	1187	1178	C-C		
	---	440			
	---	81			

[a] Least square empirical force constants: three force constants fit to six observed frequencies.

[b] Solid state multiplets were averaged for the force constant calculations.

motions is necessary. Dipole moments can be obtained if the cartesian coordinates of the equilibrium configuration are known relative to the cartesian coordinates of the system distorted by one normal coordinate unit.

The transformation from nuclear-centered cartesian displacement coordinates to internal coordinates is given as

$$R = BX \tag{2.1}$$

where the elements of the B-matrix are calculated by well known means (54) from a consideration of the molecular geometry. B is a non-square matrix so the inverse transformation cannot be obtained by simple matrix inversion.

Let the inverse transformation be given as

$$X = AR \ . \tag{2.2}$$

Inspection of Equations (2.1) and (2.2) shows that the product AB must yield the identity matrix. The following relationship is well known

$$G = BM^{-1}B^{t} \tag{2.3}$$

where G is usually referred to as the kinetic energy matrix, M^{-1} is a diagonal matrix of the reciprocals of the atomic masses, and B^{t} represents the matrix transpose of B.

Now left-multiply Equation (2.3) by A to obtain

$$AG = ABM^{-1}B^{t} \tag{2.4}$$

Right-multiplication of Equation (2.4) by G^{-1} then leads to

$$A = M^{-1}B^{t}G^{-1} \tag{2.5}$$

But $G = LL^{t}$, where L is the matrix that transforms from normal

coordinates, Q, to the internal coordinate, R. Using this result to obtain an expression for G^{-1} followed by substitution into Equation (2.5) yields

$$A = M^{-1}B^{t}(L^{-1})^{t}L^{-1} \tag{2.6}$$

Combining Equations (2.2) and (2.6) gives

$$X = M^{-1}B^{t}(L^{-1})^{t}L^{-1}R \tag{2.7}$$

Recognition of the fact that R = LQ and substitution of this into Equation (2.7) then gives the desired result that

$$X = M^{-1}B^{t}(L^{-1})^{t}Q = CQ \tag{2.8}$$

Equation (2.8) indicates, then, that the C-matrix is a rectangular matrix with dimensions 3Nx2N-3 if there are N atoms, and only planar vibrations are considered. The element in the i^{th} row and j^{th} column of the C-matrix then gives $\frac{\partial X_i}{\partial Q_i}$. The elements of a particular column in C, say the k^{th}, give the nuclear-centered cartesian displacements of the atoms for unit displacement of the k^{th} normal mode.

Generally, the L-matrix is obtained as the matrix which diagonalizes the GF-matrix by a similarity transformation. In many cases, as is the case with TCNE, there will be more internal coordinates than there are planar normal modes. In these cases, the resulting L-matrix is non-square and the inverse required in Equation (2.8) cannot be obtained directly. Diagonalization of the FG product matrix, however, yields $(L^{-1})^{t}$ directly.

A computer program was written to carry out the diagonalization of FG. Program input consists, essentially, of the F, G, and U (transforms from internal to symmetry coordinates) matrices. The program output

yields L, L^{-1}, $\mathcal{L}$, $\mathcal{L}^{-1}$, G^{-1}, X and the vibrational frequencies. $\mathcal{L}$ and $\mathcal{L}^{-1}$ represent the symmetrized L and L^{-1} matrices respectively. Various checks on the solution were also printed. The checks were incorporated primarily to insure that the L and L^{-1} matrices were properly normalized. If the L-matrix is correctly normalized, then, as shown by Crawford and Fletcher (55), the following equations must hold:

$$LL^t = G \tag{2.9}$$

as was mentioned earlier, and

$$L^tFL = \Lambda \tag{2.10}$$

where Λ is a diagonal matrix of the frequency parameters. The L^{-1} matrix was used to calculate G^{-1} and then the product of G and G^{-1} was checked to be certain that the identity matrix was obtained; this serves as a check on the correctness of L^{-1}. The product of L with L^{-1} was also checked.

The results of the cartesian displacement calculations for the neutral and anionic TCNE b_{1u} and b_{2u} C-C stretching modes are presented in Tables IV-VII. The forms of these normal modes may be determined by referring to Figure 1, which gives the atom numbering scheme. A quick check on the cartesian displacements is that the molecular center of mass remains stationary. The forms of the molecular distortions may be obtained by simply adding the nuclear-centered cartesian displacements to the appropriate cartesian coordinates of the undistorted molecule. This procedure is used to obtain the dipole moment derivatives.

TABLE IV

CARTESIAN DISPLACEMENTS IN THE b_{1u} CARBON SINGLE-BOND STRETCHING MODE IN THE NEUTRAL MOLECULE

ATOM	X(Å)	Y(Å)	Z(Å)
1	0.0000	0.0512	-0.0201
2	0.0000	-0.0512	-0.0201
3	0.0000	0.0004	-0.0595
4	0.0000	-0.0004	-0.0595
5	0.0000	0.0000	0.1659
6	0.0000	0.0000	0.1659
7	0.0000	-0.0004	-0.0595
8	0.0000	0.0004	-0.0595
9	0.0000	-0.0512	-0.0201
10	0.0000	0.0512	-0.0201

TABLE V

CARTESIAN DISPLACEMENTS IN THE b_{2u} CARBON SINGLE-BOND STRETCHING MODE IN THE NEUTRAL MOLECULE

ATOM	X(Å)	Y(Å)	Z(Å)
1	0.0000	0.0553	-0.0345
2	0.0000	0.0553	0.0345
3	0.0000	0.0230	-0.0056
4	0.0000	0.0230	0.0056
5	0.0000	-0.1750	0.0000
6	0.0000	-0.1750	0.0000
7	0.0000	0.0230	0.0056
8	0.0000	0.0230	-0.0056
9	0.0000	0.0553	0.0345
10	0.0000	0.0533	-0.0345

TABLE VI

CARTESIAN DISPLACEMENTS IN THE b_{1u} CARBON-SINGLE-BOND STRETCHING MODE IN THE ANION

ATOM	X(Å)	Y(Å)	Z(Å)
1	0.0000	0.0534	-0.0218
2	0.0000	-0.0534	-0.0218
3	0.0000	0.0013	-0.0573
4	0.0000	-0.0013	-0.0573
5	0.0000	0.0000	0.1654
6	0.0000	0.0000	0.1654
7	0.0000	-0.0013	-0.0573
8	0.0000	0.0013	-0.0573
9	0.0000	-0.0534	-0.0218
10	0.0000	0.0534	-0.0218

TABLE VII

CARTESIAN DISPLACEMENTS IN THE b_{2u} CARBON-SINGLE-BOND STRETCHING MODE IN THE ANION

ATOM	X(Å)	Y(Å)	Z(Å)
1	0.0000	0.0573	-0.0355
2	0.0000	0.0573	0.0355
3	0.0000	0.0200	-0.0043
4	0.0000	0.0200	0.0043
5	0.0000	-0.1738	0.0000
6	0.0000	-0.1738	0.0000
7	0.0000	0.0200	0.0043
8	0.0000	0.0200	-0.0043
9	0.0000	0.0573	0.0355
10	0.0000	0.0573	-0.0355

CHAPTER III

THE THEORETICAL PROBLEM

Dipole Moment Derivatives and the Perturbation Calculation

In Chapter I, a discussion of how perturbation theory can be applied to derive equations for the calculation of vibronic contributions to infrared intensities was given. The purpose of this chapter is to present a detailed account of how the expressions can be evaluated. The estimation of the π-electronic contributions to infrared intensities through calculation of dipole moment derivatives will also be discussed.

To begin with, it might be useful to review the relevant intensity equations. The vibrational intensity may be given in two possible forms as is indicated by the following equation:

$$\Gamma_i = \frac{N\pi}{3c^2\bar{\nu}_i}\left(\frac{\partial\vec{\mu}}{\partial Q_i}\right)^2_{Q_i=0} = \frac{8\pi^3 N}{3hc}\left|\vec{M}_{go,gi}\right|^2 \qquad (3.1)$$

It is therefore clear that the capability of calculating vibrational intensities rests in the ability to estimate either the dipole moment derivative, $\frac{\partial\vec{\mu}}{\partial Q_i}$, or, the vibrational transition moment, $\vec{M}_{go,gi}$.

The quantity $\frac{\partial\vec{\mu}}{\partial Q_i}$ can, of course, be obtained most easily by simply distorting the molecule away from its equilibrium configuration - in a manner appropriate for the i^{th} normal coordinate - and doing a complete

quantum mechanical calculation in this distorted geometry. The arrangement of electron density in the distorted configuration relative to that obtained for the equilibrium geometry produces a new dipole moment; distortion followed by calculation of electron densities thus yields $\vec{\mu}$ as a function of Q, and, hence, leads to an estimate of the dipole moment derivative.

It is well known that the dipole moment of a system that bears a net charge is dependent upon the choice of the coordinate system origin. At first thought, one might expect that this result makes it impossible to calculate a unique dipole moment derivative - for the anion - by the techniques mentioned above. Actually, changes in the dipole moment of a charged system can be shown to be independent of the choice of origin.

Consider writing the x-component of the dipole moment of a system containing N atoms as

$$\mu_x = \sum_{i=1}^{N} q_i x_i \tag{3.2}$$

where q_i and x_i are, respectively, the charge and x-coordinate of the i^{th} atom. Now translate the whole system along the x-axis by an amount of Δx. The new dipole moment, μ_x', now becomes

$$\mu_x' = \sum_{i=1}^{N} q_i x_i + \Delta x \sum_{i=1}^{N} q_i \tag{3.3}$$

Equation (3.3) above shows that, for a charged system, the dipole moment is dependent upon the choice of the coordinate system origin since the sum of the q_i is not zero. Now by taking the differentials of Equations (3.2) and (3.3) the following results are obtained

$$d\mu_x = \sum_{i=1}^{N} (x_i dq_i + q_i dx_i) \tag{3.4}$$

and

$$d\mu'_x = d\mu_x + \Delta x \sum_{i=1}^{N} dq_i \qquad (3.5)$$

But, since the total charge is conserved, the sum of the dq_i must be zero; therefore, the change in the dipole moment of a charged system is independent of the choice of an origin.

Several authors have applied the quantum mechanical dipole moment derivative approach (56-60). All papers have employed the complete neglect of differential overlap (CNDO) method. As is evident from Equation (3.1), the experimental measurement of the infrared intensity yields no information about the actual algebraic sign of the dipole moment derivative; CNDO - type calculations, however, allow a choice to be made as to the actual signs of the derivatives.

The CNDO method mentioned earlier explicitly considers all of the valence electrons. In this study, however, only the π-electrons will be accorded explicit consideration. The rationale behind this approach is based on the belief that the gross spectral differences that exist between the neutral and anionic TCNE molecules are due primarily to differences in the π-electron systems of the two species. The plan is to investigate changes in the π-electronic moments of the two molecules as they are distorted. This information, coupled with an estimate of the effect of vibration on the framework (i.e. the nuclei and σ-electronic system) dipole moment, should then allow an estimate to be made of the effect on the vibrational intensities produced by the radical electron. This approach is based on the assumption that the framework contribution to the dipole moment derivative remains essentially constant in both the neutral and anionic molecular systems. Any changes in

infrared band intensities in the two systems can, therefore, be taken as being due to different π-electronic contributions in the two systems.

The second approach to be used in this study is based on the Herzberg-Teller theory. This method is particularly interesting in that it relates high vibrational intensities to high electronic intensities. An insight into how infrared intensities and electronic transition intensities can be coupled to yield molecular force field data is also achieved. The rest of this chapter is concerned with the derivation of the expressions necessary to implement a Herzberg-Teller type calculation.

In Chapter I, it was shown how nuclear coordinate dependence could be introduced into the electronic wave function. The approach was to consider the nuclear motions as being small perturbations on the wave functions calculated at the equilibrium geometry. First order perturbation theory was then utilized to obtain the perturbed wave functions. It was then shown how the π-electronic-vibronic contribution to the total vibrational transition moment could be obtained from the vibronic wave functions. The end result of that analysis led to the following equation for the vibronic contribution to the i^{th} vibrational mode.

$$\vec{M}_{go,gi} = -2\left(\frac{h}{8\,{}^{2}C\bar{\nu}_i}\right)^{\frac{1}{2}} \sum_{j\neq g} \frac{\langle \psi_j{}^{o} \left| \frac{\partial H}{\partial Q_i} \right| \psi_g{}^{o} \rangle}{E_j{}^{o} - E_g{}^{o}} \langle \psi_g{}^{o} | \vec{P}op | \psi_j{}^{o} \rangle \qquad (3.6)$$

$\vec{M}_{go,gi}$ represents the π-electron transition moment for a transition from the ground electronic, ground vibrational state to the ground electronic state with one quantum of excitation in the i^{th} normal mode. The only quantity in Equation (3.6) that is not an experimentally observable parameter is the perturbation integral. It can be seen, however, how

this quantity could be obtained from analysis of vibrational and electronic transition intensities along with electronic transition energies. Inspection of Equation (1.18) illustrates how information regarding contributions to the resonance force field can also be obtained from this analysis.

Since the only reliable experimental data obtained in this study are of a vibrational spectroscopic nature, it was essential to seek information regarding the electronic spectra of neutral and anionic TCNE. From Equation (3.6), it may be seen that the relevant data are the electronic transition energies and the associated transition moments. Estimates of the perturbation integrals are also required in conjunction with the electronic spectral data since these quantities determine the π-electronic contributions to the various infrared transition moments. As pointed out in the first chapter, it is believed that the grossest intensity effects (apart from the activation of normally IR-inactive modes) in the neutral and anionic molecules occur in the b_{1u} and b_{2u} carbon-carbon single bond stretches. These modes will be treated in detail.

The molecular oribtal theory will be used to calculate the electronic transition energies, electronic transition moments, and the perturbation integrals. The contributions of the π-electronic moments predicted by this method will then be used to make qualitative predictions about infrared intensities in anionic TCNE relative to the intensities in the neutral molecule.

A Pariser-Parr-Pople-type (61) (62) calculation will be done to obtain the molecular wave functions along with the electronic transition energies and associated moments. The calculations will be of the

self-consistent-field (SCF) type and will consider limited configuration interaction (CI). Only those excited states produced by the excitation of a single electron will be considered. The computer program written to perform these calculations is capable of handling either open- or closed-shell systems (63) (64). Only the π-electrons are explicitly considered and all multi-cneter integrals are reduced to one- and two-center integrals through the zero-differential-overlap (ZDO) assumption. Coulomb integrals, bond resonance integrals, and electron repulsion integrals are all evaluated semi-empirically.

Several references (65-67) have served as guidelines for the present calculations. Particular choices of computational procedures and semi-empirical parameters have been obtained from these papers. The justification for the incorporation of a particular value or form for a given parameter is based on how well experimental data are reproduced by the calculation when that particular value is used. Computed transition energies and intensities, ionization potentials, electron affinities, etc. will be compared with experiment as an aid in judging the sufficiency of the calculation.

Once an acceptable wave function has been determined, calculations of the vibrational perturbation integrals, and, ultimately the π-electronic contribution to the vibrational moments can be undertaken. The approach used here follows calculations presented by Donath (20) (21), Brown (30), and more recently by Roche and Jaffe (68).

Consider expanding the molecular electronic Hamiltonian in a Taylor's series with respect to the normal coordinates, Q_a. Retention of only those terms linear in the Q_a leads to

$$H(Q) = H(Q_o) + \sum_{a=1}^{3N-6} \left(\frac{\partial H}{\partial Q_a}\right)_0 Q_a \ . \qquad (3.7)$$

Hereafter, $H(Q)$ and $H(Q_0)$ will be written as H and H_0 respectively. If N represents the number of atoms of a non-linear molecule, then there are 3N-6 degrees of vibrational freedom. All partial derivatives are evaluated at the equilibrium values of the Q_a (e.g. $Q_a = 0$).

Now, the wave functions are assumed to be known for the equilibrium configuration, i.e.

$$H_0\psi_k^0 = E_k^0\psi_k^0 \qquad (3.8)$$

Substitution for H_0 from Equation (3.7) followed by left multiplication by the complex conjugate of ψ_j^0 and integration over all electronic space leads to

$$\langle\psi_j^0|H|\psi_k^0\rangle - \sum_{a=1}^{3N-6}\langle\psi_j^0|\frac{\partial H}{\partial Q_a}|\psi_k^0\rangle Q_a = E_k^0\langle\psi_j^0|\psi_k^0\rangle \qquad (3.9)$$

since, as was mentioned in the first chapter, $\frac{\partial H}{\partial Q_a}$ is a one-electron operator. Considering the case when $j \neq k$ followed by differentiation of Equation (3.9) with respect to any normal coordinate, say Q_b, yields

$$\frac{\partial}{\partial Q_b}\langle\psi_j^0|H|\psi_k^0\rangle = \langle\psi_j^0|\frac{\partial H}{\partial Q_b}|\psi_k^0\rangle \qquad (3.10)$$

Equation (3.6) is perfectly general as long as the ψ_j^0 are independent of the Q_b. The integral appearing on the left-hand side of Equation (3.10) is recognized as a CI-type integral. Thus, as may be seen from Equation (3.10), the perturbation integral can be obtained by evaluating the derivative, with respect to a normal coordinate, of a CI-matrix

element. The only CI-matrix elements to be considered in this study will be those between the ground electronic state and those excited states formed by single-electronic excitations.

It should be pointed out that if the molecular orbitals obtained in the calculations are really self-consistent, Brillouin's theorem (69) applies. It states that all matrix elements between the ground state and excited states of the type considered here are identically zero. This is true, however, only for the configuration for which the SCF calculation was performed (usually the equilibrium geometry is used). Brillouin's theorem does not hold when the Q_a are different from zero, since the molecular orbitals are no longer self-consistent. The expressions for the derivatives of the ground state-excited state interaction elements must, therefore, be obtained.

Donath (21) gives a general expression for the interaction element between the ground electronic state and a singly excited state. The ground state wave function is approximated as a single Slater determinant. For a 2N-electron system, $\bar{\Psi}_g$, the ground state wave function, will be represented as

$$\bar{\Psi}_g = |\psi_1\bar{\psi}_1\cdots\psi_i\bar{\psi}_i\cdots\psi_N\bar{\psi}_N| \tag{3.11}$$

where no bar indicates an electron with α-spin, and a bar represents an electron with β-spin. The excited state wave function, where an electron in the i^{th} doubly occupied molecular orbital has been promoted to the k^{th} virtual orbital, can be given as

$$\bar{\Psi}_{i\to k} = \frac{1}{\sqrt{2}}\left(|\psi_1\bar{\psi}_1\cdots\psi_k\bar{\psi}_i\cdots\psi_N\bar{\psi}_N| + |\psi_1\psi_1\cdots\psi_i\bar{\psi}_k\cdots\psi_N\bar{\psi}_N|\right). \tag{3.12}$$

Using the general rules governing integrals between Slater determinants

and performing the integration over spin coordinates, leads to the following expression

$$\langle \bar{\Psi}_g | H | \bar{\Psi}_{i\to k} \rangle = \sqrt{2}\left[\langle \psi_i | H^{core} | \psi_k \rangle + \sum_{j=1}^{N} 2\langle \psi_i \psi_j | G | \psi_k \psi_j \rangle - \langle \psi_i \psi_j | G | \psi_j \psi_k \rangle\right] \quad (3.13)$$

where

$$\langle \psi_i \psi_j | G | \psi_k \psi_j \rangle \equiv \langle \psi_i(1)\psi_j(2) | \frac{e^2}{r_{12}} | \psi_k(1)\psi_j(2) \rangle \quad (3.14)$$

H^{core} is a sum of one-electron operators which represent the kinetic energy of an electron plus its potential interaction with the nuclear and σ-electronic systems. It should be noted that the sum in Equation (3.13) is over all molecular orbitals that are doubly occupied in the ground state.

Since molecular orbitals are formed from linear combinations of atomic orbitals (LCAO), Equation (3.13) may be reduced to integrals over atomic orbitals. This reduction along with the ZDO approximation transforms Equation (3.13) into

$$\langle \bar{\Psi}_g | H | \bar{\Psi}_{i\to k} \rangle = \sqrt{2}\left(\sum_{m=1}^{2N} C_{km}C_{im}\alpha_m + \sum_{m=1}^{2N}\sum_{n=1}^{2N} C_{km}C_{in}\beta_{mn} + 2\sum_{m=1}^{2N}\sum_{n=1}^{2N} C_{km}C_{im}\sum_{j=1}^{N} C_{jn}^2\gamma_{mn} - \sum_{m=1}^{2N}\sum_{n=1}^{2N} C_{km}C_{in}\sum_{j=1}^{N} C_{jm}C_{jn}\gamma_{mn}\right) \quad (3.15)$$

In Equation (3.15), C_{pq} represents the linear combination coefficient of the q^{th} atomic orbital in the p^{th} molecular orbital. The quantities α_m and β_{mn} are the diagonal and off-diagonal matrix elements of H^{core} respectively. α_m and β_{mn} are often called coulomb and resonance integrals respectively. The γ_{mn} represents the two-center electron repulsion integrals between centers m and n.

Henceforth, it should be understood that when no upper limit appears on a summation, that sum runs over all 2N atomic centers. Similarly, only the index of the summation will be written since all sums begin with an index of unity.

At this point it becomes necessary to make a commitment as to how the various semi-empirical parameters are to be evaluated. Since the derivative of Equation (3.15) with respect to a normal coordinate must be taken, it is mandatory to know the explicit dependence of the parameter on the internuclear distances.

The semi-empirical parameter approximations to be used in this study are fairly standard. For instance, the two-center electron repulsion integrals will be calculated according to the Mataga-Nishimoto formula (71)

$$\gamma_{\mu\nu} = \frac{a_{\mu\nu}}{1+.06944 a_{\mu\nu} R_{\mu\nu}} \tag{3.16}$$

where

$$a_{\mu\nu} = \tfrac{1}{2}(\gamma_{\mu\mu} + \gamma_{\mu\mu}) \tag{3.17}$$

and $\gamma_{\mu\mu}$ is obtained as

$$\gamma_{\mu\mu} = I_{\mu} - A_{\mu} \tag{3.18}$$

I_{μ} and A_{μ} are, respectively, the valence state ionization potential and electron affinity of the μ^{th} atom.

The resonance integral, $\beta_{\mu\nu}$, between bonding atomic centers μ and ν is approximated from Kuprievich

$$\beta_{\mu\nu} = -\beta_{0(\mu\nu)} \exp(-\kappa R_{\mu\nu}) \tag{3.19}$$

$\beta_{0(\mu\nu)}$ is a constant for a given type of bond and κ is a constant for all bonds in the molecule. All bond resonance integrals between centers not connected by a chemical bond are set to zero. $R_{\mu\nu}$ is the internuclear distance.

The final parameter to be defined is α_m, the diagonal matrix element of H^{core}. The definition adopted in this study has been used in the past with reasonable success and is given by

$$\alpha_m = -I_m - \sum_{n \neq m} Z_n \gamma_{mn} \tag{3.20}$$

Where Z_n represents the core charge residing on the n^{th} atomic center. All other quantities appearing in Equation (3.20) have been discussed earlier.

It now becomes expedient to discuss how the derivatives with respect to normal coordinates can be transformed to derivatives with respect to internal coordinates. This is necessary because the definitions used for the semi-empirical parameters are explicit functions of the internal coordinates, e.g. the bond lengths. Introducing the transformation between internal and normal coordinates (54) and employing the chain rule leads to

$$\frac{\partial}{\partial Q_a} = \tfrac{1}{2} \sum_{\mu} \sum_{\nu} \frac{\partial R_{\mu\nu}}{\partial Q_a} \frac{\partial}{\partial R_{\mu\nu}} \tag{3.21}$$

where terms involving valence angle bending internal coordinates have been excluded since the semi-empirical parameters are functions of the $R_{\mu\nu}$ only. The quantities $\frac{\partial R_{\mu\nu}}{\partial Q_a}$ are determined from the L-matrix which produces the transformation from normal to internal coordinates. The L-matrix is, of course, determined from a normal coordinate analysis of the molecular system. The factor of one-half is necessary since both

sums run over all centers and $R_{\mu\nu} = R_{\nu\mu}$.

Using Equation (3.21), the derivatives of the parameters which occur in Equation (3.15) can be obtained. For instance

$$\frac{\partial \beta_{mn}}{\partial Q_a} = \tfrac{1}{2} \sum_{\mu} \sum_{\nu} \frac{\partial R_{\mu\nu}}{\partial Q_a} \frac{\partial \beta_{mn}}{\partial R_{\mu\nu}} \tag{3.22}$$

and

$$\frac{\partial \alpha_m}{\partial Q_a} = - \sum_{n \neq m} Z_n \sum_{\mu} \sum_{\nu} \frac{\partial \gamma_{mn}}{\partial R_{\mu\nu}} \frac{\partial R_{\mu\nu}}{\partial Q_a} \tag{3.23}$$

The assumed forms of the parameters, β_{mn} and γ_{mn}, show that they are dependent upon one and only one bond length, namely R_{mn}. Therefore, Equations (3.22) and (3.23) may be reduced to

$$\frac{\partial \beta_{mn}}{\partial Q_a} = \kappa \beta_{mn} \frac{\partial R_{mn}}{\partial Q_a} \tag{3.24}$$

and

$$\frac{\partial \alpha_m}{\partial Q} = - \sum_{n \neq m} \frac{\partial \gamma_{mn}}{\partial R_{mn}} \frac{\partial R_{mn}}{\partial Q_a} \tag{3.25}$$

Substitution of these results into Equation (3.15) and simultaneously introducing the definition that

$$P_{mn} = 2 \sum_{j}^{N} C_{jm} C_{jn} \tag{3.26}$$

leads to the following expression

$$\frac{\partial}{\partial Q_a} \langle \psi_g | G | \psi_{i \to k} \rangle = \sqrt{2} \left(- \sum_{m} \sum_{n} C_{km} C_{in} Z_n \frac{\partial \gamma_{mn}}{\partial R_{mn}} \frac{\partial R_{mn}}{\partial Q_a} + \sum_{m} \sum_{n} \kappa C_{km} C_{in} \beta_{mn} \frac{\partial R_{mn}}{\partial Q_a} \right.$$

$$\left. + \sum_{m} \sum_{n} P_{nn} C_{km} C_{im} \frac{\partial \gamma_{mn}}{\partial R_{mn}} \frac{\partial R_{mn}}{\partial Q_a} - \sum_{m} \sum_{n} \frac{P_{mn}}{2} C_{km} C_{in} \frac{\partial \gamma_{mn}}{\partial R_{mn}} \frac{\partial R_{mn}}{\partial Q_a} \right) \tag{3.27}$$

Using Donath's definition (21) of transition density,

$$P_{mn}^{i\to k} = \frac{1}{\sqrt{2}} (C_{im}C_{kn} + C_{in}C_{km}) \tag{3.28}$$

and combining terms in Equation (3.27) results in

$$\frac{\partial}{\partial Q_a} < \bar{\psi}_g | H | \bar{\psi}_{i\to k} > = \sum_m \sum_n (P_{nn} - Z_n) P_{mm}^{i\to k} \frac{\partial \gamma_{mn}}{\partial R_{mn}} \frac{\partial R_{mn}}{\partial Q_a}$$

$$- \sqrt{2} \sum_m \sum_n C_{km} C_{in} \left(-\kappa\beta_{mn} + \frac{P_{mn}}{2} \frac{\partial \gamma_{mn}}{\partial R_{mn}}\right) \frac{\partial R_{mn}}{\partial Q_a} \tag{3.29}$$

Inspection of the second double summation in Equation (3.29) indicates that an interchange of the subscripts n and m would not affect the summation. Using this fact leads to

$$\sum_m \sum_n C_{km} C_{in} \left(-\kappa\beta_{mn} + \frac{P_{mn}}{2} \frac{\partial \gamma_{mn}}{\partial R_{mn}}\right) \frac{\partial R_{mn}}{\partial Q_a} =$$

$$\tfrac{1}{2} \sum_m \sum_n (C_{km} C_{in} + C_{im} C_{kn}) \left(-\kappa\beta_{mn} + \frac{P_{mn}}{2} \frac{\partial \gamma_{mn}}{\partial R_{mn}}\right) \frac{\partial R_{mn}}{\partial Q_a} . \tag{3.30}$$

Substitution of this result into Equation (3.29) yields

$$\frac{\partial}{\partial Q_a} <\psi_g | H | \bar{\psi}_{i\to k}> = \sum_m \sum_n (P_{nn} - Z_n) P_{mm}^{i\to k} \frac{\partial \gamma_{mn}}{\partial R} \frac{\partial R_{mn}}{\partial Q_a}$$

$$- \sum_m \sum_n \frac{1}{\sqrt{2}} (C_{km} C_{in} + C_{kn} C_{im}) \left(-\kappa\beta_{mn} + \frac{P_{mn}}{2} \frac{\partial \gamma_{mn}}{\partial R_{mn}}\right) \frac{\partial R_{mn}}{\partial Q_a} \tag{3.31}$$

Use of Equation (3.28) then produces

$$\frac{\partial}{\partial Q_a} <\bar{\psi}_g | H | \bar{\psi}_{i\to k}> = \sum_m \sum_n (P_{nn} - Z_n) P_{mm}^{i\to k} \frac{\partial \gamma_{mn}}{\partial R} \frac{\partial R_{mn}}{\partial Q_a} -$$

$$\sum_m \sum_n P_{mn}^{i\to k} \left(-\kappa\beta_{mn} + \frac{P_{mn}}{2} \frac{\partial \gamma_{mn}}{\partial R_{mn}} \frac{\partial \gamma_{mn}}{\partial R_{mn}}\right) \frac{\partial R_{mn}}{\partial Q_a} . \tag{3.32}$$

Inspection of Equation (3.32) bears out an observation made by Jones (32) that the transition densities are sufficient to determine the perturbation integral. Fischer-Hjalmers (72) presents a discussion on the use of transition densities between the ground and excited states in qualitative studies of the intensities of forbidden electronic transitions.

The foregoing derivation of the perturbation integral was concerned solely with systems with closed-shell ground states. The goal of this study is to compare theoretical values of the vibrational transition moments of the neutral molecule with the corresponding moments of the anion. It therefore becomes necessary to develop an expression equivalent to Equation (3.32) for cases when the ground state is not a closed shell system (i.e. the anion). The reason for presenting a detailed derivation of the expression given by Donath (21) is that the derivation of the corresponding expressions for open-shell systems will proceed in an analogous manner.

The decision has been made to consider only two types of transitions: a) transitions from a doubly occupied orbital to the orbital containing the radical electron; and b) transitions of the radical electron to a virtual orbital. These transitions are expected to be the lowest energy ones and, due to the appearance of the excitation energy in the denominator of Equation (3.6), should produce the largest contributions to the vibrational transition moment.

Let the doublet ground state of the anion be represented by

$$^2\underline{\bar{\psi}}_g = |\psi_1\bar{\psi}_1 \cdots \psi_i\bar{\psi}_i \cdots \psi_N\bar{\psi}_N\psi_{N+1}| \qquad (3.33)$$

The wave functions for the two types of excited states to be considered in this study can then be written as:

$$\text{Type a)} \quad {}^{2}\bar{\Psi}_{i\to N+1} = |\psi_1\bar{\psi}_1\cdots\psi_i\bar{\psi}_{N+1}\cdots\psi_N\bar{\psi}_N\psi_{N+1}| \tag{3.34}$$

and

$$\text{Type b)} \quad {}^{2}\bar{\Psi}_{N+1\to k} = |\psi_1\bar{\psi}_1\cdots\psi_i\bar{\psi}_i\cdots\psi_N\bar{\psi}_N\psi_k| \tag{3.35}$$

In Equation (3.35) it should be emphasized that the molecular orbital subscript, k, labels a spatial orbital not occupied in the ground state.

Longuet-Higgins and Pople (21) have provided the necessary integral expressions for the two types of transitions being considered here. Their results yield (after integration over the spin coordinates)

$$\langle {}^{2}\bar{\Psi}_g|H|\bar{\Psi}_{i\to N+1}\rangle = \langle\psi_i|H^{core}|\psi_{N+1}\rangle + \sum_{j=1}^{N}[2\langle\psi_j\psi_i|G|\psi_j\psi_{N+1}\rangle - \langle\psi_j\psi_i|G|\psi_{N+1}\psi_j\rangle]$$

$$+ \langle\psi_{N+1}\psi_i|G|\psi_{N+1}\psi_{N+1}\rangle \tag{3.36}$$

and

$$\langle {}^{2}\bar{\Psi}_g|H|\bar{\Psi}_{N+1\to k}\rangle = \langle\psi_{N+1}|H^{core}|\psi_k\rangle + \sum_{j=1}^{N}[2\langle\psi_j\psi_{N+1}|G|\psi_j\psi_k\rangle - \langle\psi_j\psi_{N+1}|G|\psi_k\psi_j\rangle] \tag{3.37}$$

An explanation of the notation used in Equations (3.36) and (3.37) is given earlier in this chapter.

Apart from an additional term occurring in Equation (3.36), inspection shows Equations (3.36) and (3.37) contain terms identical in form. Those terms are of the following type

$$\langle\psi_p|H^{core}|\psi_q\rangle + [\sum_{j=1}^{N} 2\langle\psi_j\psi_p|G|\psi_j\psi_q\rangle - \langle\psi_j\psi_p|G|\psi_q\psi_j\rangle] \tag{3.38}$$

A derivation of the derivative with respect to a normal coordinate of the expression given in Equation (3.38) will now be undertaken. The derivation is, as would be expected, very similar to that presented for the case when the molecular ground state is a closed-shell system.

Reduction of Equation (3.38) to integrals over atomic orbitals and, once again invoking the ZDO approximation, yields

$$\langle\psi_p|H^{core}|\psi_q\rangle + \left[\sum_{j=1}^{N} 2\langle\psi_j\psi_p|G|\psi_j\psi_q\rangle - \langle\psi_j\psi_p|G|\psi_q\psi_j\rangle\right] =$$

$$\sum_m C_{pm}C_{qm}\alpha_m + \sum_m\sum_n C_{pm}C_{qn}\beta_{mn} + 2\sum_m\sum_n C_{pn}C_{qn}\sum_{j=1}^{N} C_{jm}^2\gamma_{mn}$$

$$- \sum_m\sum_n C_{pm}C_{qn}\sum_{j=1}^{N} C_{jm}C_{jn}\gamma_{mn} \qquad (3.39)$$

Apart from a factor of $\sqrt{2}$, Equation (3.39) is identical to Equation (3.11). The atomic orbital coefficients are, of course, different from those in Equation (3.15), since those used in Equation (3.39) are the coefficients which minimize the total energy of the open-shell ground state. Making use of the fact that Equation (3.39) is identical in form to Equation (3.15), plus the fact that all arguments used in evaluating the derivative of Equation (3.15) also apply to obtaining the derivative of Equation (3.39), leads to

$$\frac{\partial}{\partial Q_a}\left\{\langle\psi_p|H^{core}|\psi_q\rangle + \left[\sum_{j=1}^{N} 2\langle\psi_j\psi_p|G|\psi_j\psi_q\rangle - \langle\psi_j\psi_p|G|\psi_q\psi_j\rangle\right]\right\} =$$

$$\frac{1}{\sqrt{2}}\left[\sum_m\sum_n (P_{nn}^c - Z_n) P_{mm}^{p\to q}\frac{\partial\gamma_{mn}}{\partial R_{mn}}\frac{\partial R_{mn}}{\partial Q_a} - \sum_m\sum_n P_{mn}^{p\to q}\left(-\kappa\beta_{mn} + \frac{P_{mn}^c}{2}\frac{\partial\gamma_{mn}}{\partial R_{mn}}\right)\frac{\partial R_{mn}}{\partial Q_a}\right]$$

(3.40)

The quantities denoted as P_{mn}^c which appear in Equation (3.40) are

defined as

$$P^{c}_{mn} = 2 \sum_{j=1}^{N} C_{jm} C_{jn} \tag{3.41}$$

and are elements of the closed-shell density matrix. This is not the total density matrix since the singly occupied molecular orbital is not included in the summation. The $P^{p\to q}_{mn}$ are as defined in Equation (3.28).

It must be noted that when the transition occurs from a doubly occupied orbital, ψ_i, to the singly occupied orbital, ψ_{N+1}, another term arises whose derivative must be evaluated. That term is

$$\langle \psi_{N+1}\psi_i | G | \psi_{N+1}\psi_{N+1} \rangle = \sum_m \sum_n C^2_{N+1,m} C_{N+1,n} C_{in} \gamma_{mn} \tag{3.42}$$

Now let

$$C^2_{N+1,m} = P^{O}_{mm} \tag{3.43}$$

where P^{O}_{mm} is a diagonal element of the density matrix for the open shell. By introducing the definition of the transition densities, Equation (3.42) can be written as

$$\sum_m \sum_n C^2_{N+1,m} C_{N+1,n} C_{in} \gamma_{mn} = \frac{1}{\sqrt{2}} \sum_m \sum_n P^{O}_{mm} P^{i\to N+1}_{nn} \gamma_{mn} \tag{3.44}$$

The derivative of Equation (3.40) can be easily obtained. Therefore, the desired result for all transitions either to or from the molecular orbital containing the radical electron can be summarized as follows:

$$\frac{\partial}{\partial Q_a} \langle {}^2\bar{\psi}_g | G | {}^2\bar{\psi}_{p\to q} \rangle = \frac{\sqrt{2}}{2} \Big[\sum_m \sum_n (P^{c}_{nn} - Z_n) P^{p\to q}_{mm} \frac{\partial \gamma_{mn}}{\partial R_{mn}} \frac{\partial R_{mn}}{\partial Q_a} -$$

$$\sum_m \sum_n P^{p\to q}_{mn} \left(-\kappa \beta_{mn} + \frac{P^{c}_{mn}}{2} \frac{\partial \gamma_{mn}}{\partial R_{mn}}\right) \frac{\partial R_{mn}}{\partial Q_a} + \delta_{q,N+1} \sum_m \sum_n P^{O}_{mm} P^{p\to q}_{nn} \frac{\partial \gamma_{mn}}{\partial R_{mn}} \frac{\partial R_{mn}}{\partial Q_a} \Big] \tag{3.45}$$

The foregoing equation is valid only when either p or q represents the molecular orbital containing the radical electron, i.e. the $(N+1)^{th}$ orbital. The quantity $\delta_{q,N+1}$ is non-zero only for transitions from a doubly occupied molecular orbital to the singly occupied orbital - a result indicated by the forms of Equations (3.36) and (3.37).

It should be pointed out that the $\frac{\partial R_{mn}}{\partial Q_a}$ appearing in Equation (3.45) should be determined from a normal coordinate analysis of the anion. The derivatives of the γ_{mn} are easily obtained from a simple differentiation of Equation (3.16). The β_{mn} are also readily available, and the matrices $P^{p\to q}$, P^c, and P^o are obtained in the SCF calculation.

Equations (3.32) and (3.45) can then be applied to estimate the π-electronic-vibronic contributions to the infrared transition moments for the neutral and anionic molecules respectively. These contributions, together with an estimate of the framework contribution to the transition moment, can be used to make at least qualitative predictions of vibrational intensities in the anion relative to those in the neutral molecule. The framework contribution can then be estimated by assuming that the total transition moment consists of the sum of the framework contribution and the π-electronic contribution.

Force Constants

In this section, an attempt will be made to derive an equation relating bond stretching force constants to the elements of the density matrix. The force constant for a particular bond can be obtained by evaluating the second derivative of the total electronic energy of the system.

Following Bratosz and Besnainou (74) the electronic energy may be written as

$$E = \frac{1}{2} \sum_m \sum_n \sigma_{mn} + \sum_m P_{mm}\left[\alpha_m + \frac{1}{4} P_{mm}\ _{mm}\right] + \sum_m \sum_n P_{mn}\ \beta_{mn} \quad +$$

$$\frac{1}{2} \sum_m \sum_n (P_{mm}\ P_{nn} - P_{mm} - P_{nn} - \frac{1}{2} P_{mn}^2)\ \gamma_{mn} \tag{3.46}$$

The quantity σ_{mn} gives the contribution of the σ-electrons to the total energy.

Now consider the case of a pure singly bonded diatomic molecule; this case implies $P_{11} = P_{22} = 1$ and $P_{12} = 0$. A pure doubly bonded molecule would imply $P_{11} = P_{22} = 1$ and $P_{12} = 1$. A pure triply bonded molecule would lead to $P_{11} = P_{22} = 1$ and $P_{12} = 2$. Using these results in Equation (3.46) leads to

$$E_s = \sigma_{12} - \gamma_{12} + C_1 \tag{3.47}$$

and

$$E_d = \sigma_{12} + 2\beta_{12} - \frac{3}{2} \gamma_{12} + C_2 \tag{3.48}$$

and similarly

$$E_t = \sigma_{12} + 4\beta_{12} - 3\gamma_{12} + C_3 \tag{3.49}$$

C_1, C_2, and C_3 represent terms that are independent of bond length; and, since derivatives with respect to bond lengths are to be taken, these terms will yield zeroes and will therefore be dropped.

E_s, E_d, and E_t may also be defined by the following equations

$$E_s = \frac{1}{2} K_s\ (R_{12} - s)^2 \tag{3.50}$$

$$E_d = \frac{1}{2} K_d\ (R_{12} - d)^2 \tag{3.51}$$

$$E_t = \frac{1}{2} K_t (R_{12} - t)^2 \tag{3.52}$$

where s, d, and t represent the equilibrium bond lengths for pure single, double, and triple bonds respectively. K_s, K_d, and K_t represent force constants for these bonds.

Combining Equations (3.47) - (3.49) with Equations (3.50) - (3.52) leads to three non-homogeneous linear equations in three unknowns. Solution of this set of equations yields

$$\sigma_{12} = K_d(R_{12} - d)^2 - \frac{1}{2} K_t(R_{12} - t)^2 \tag{3.53}$$

$$\beta_{12} = -\frac{3}{8}K_s(R_{12} - s)^2 + \frac{1}{2} K_d(R_{12} - d)^2 - \frac{1}{8} K_t(R_{12} - t)^2 \tag{3.54}$$

$$\gamma_{12} = -\frac{1}{2} K_s(R_{12} - s)^2 + K_d(R_{12} - d)^2 - \frac{1}{2} K_t(R_{12} - t)^2 \tag{3.55}$$

Substitution of Equations (3.53) - (3.55) into Equation (3.46) followed by taking the second derivative with respect to a particular bond length would then yield a force constant. Several simplifying assumptions can be made first, however. It has been shown that neglect of the contributions to the derivatives due to the α_m and P_{mn} greatly simplifies the task and produces negligible error (74). With this in mind, an expression for a stretching force constant between centers m and n can be extracted. The result is

$$k_{mn} = 2K_d - K_t + 2P_{mn}(-\frac{3}{4} K_s + K_d - \frac{1}{4} K_t)$$

$$+ (P_{mm} P_{nn} - P_{mm} - P_{nn} - \frac{1}{2} P_{mn}^2)(-K_s + 2K_d - K_t) \tag{3.56}$$

Equation (3.56) will be used to estimate force constants in the neutral

and anionic molecules. The stretching force constant differences between the two systems will, hopefully, bolster the arguments used in assigning the infrared spectrum of the anion.

CHAPTER IV

RESULTS AND DISCUSSION

In this chapter numerical estimates of the π-electron contributions to the infrared transition moments will be made. Two methods for implementing these calculations were discussed in the previous chapter. The first method was concerned with the computation of charge densities at the equilibrium nuclear configuration and at a configuration appropriate for unit displacement in the normal coordinate being considered. This procedure allows estimates of the dipole moment derivative. The second method is based on the Herzberg-Teller formalism (15) which utilizes first-order perturbation theory to introduce nuclear coordinate dependence into the ground state wave function. The new wave function is then used to evaluate the desired infrared transition moment integrals. A discussion of the relative reliabilities of the two approaches will be undertaken. The first step is to obtain reliable wave functions for the neutral molecule and the anion.

Calculation of the Ground State Wave Functions

A Pariser-Parr-Pople formalism (61) (62) was used to obtain the ground state wave functions used in this study. Limited configuration interaction (CI) was considered between the nine lowest-energy singly excited states of the neutral molecule and between seven of the lowest-energy singly excited states of the anion. It should be pointed

out that CI does not affect the ground state wave functions in either the neutral or anionic molecules. A discussion of the evaluation of the Hartree-Fock matrix elements will be relegated to the Appendix.

The forms of the semi-empirical parameters which were incorporated into the calculation were discussed in the preceding chapter. A discussion of the evaluation of the semi-empirical parameters will now be undertaken. The valence state ionization potentials (I_μ) and electron affinities (A_μ) used in the evaluation of the electron repulsion integrals ($\gamma_{\mu\nu}$) and the diagonal elements of H^{core} were obtained from the work of Hinze and Jaffe (74). The actual values are 14.18 eV and 1.66 eV for the ionization potential and electron affinity for nitrogen and 11.16 eV and 0.03 eV for the respective carbon values.

It seemed to be a reasonable first approximation to use the same bond resonance integrals in TCNE that Lowitz (65) incorporated into a similar calculation of the electronic spectra of tetracyanoquinodimethane (TCNQ) and its anion. Lowitz (65) used resonance integrals that were proportional to the orbital overlap. The best fit to the experimental data was provided by: $\beta_{CN} = -3.6$ eV at 1.158 A, and $\beta_{CC} = -2.39$ eV at 1.39 A. Resonance integrals between atoms not connected by a chemical bond were set to zero. In this study, the bond resonance integrals are related to the bond lengths through a decaying exponential function. The pre-exponential factors were chosen to reproduce the TCNQ resonance integrals at the internuclear distances given by Lowitz (65). The structure of the neutral TCNE molecule is given in Figure 1. Due to the lack of any X-ray drystallographic data for the TCNE anion, its structure was assumed to be the same as that presented for the neutral molecule. This assumption is also supported by the

experimental observation that the anion is formed without severe structural modifications (4).

Table VIII gives the eigenvalues and molecular orbitals calculated for neutral TCNE. Also included in the table are the irreducible representations to which each molecular orbital belongs. This group theoretical classification of the molecular orbitals yields information about ground and excited state symmetries. Furthermore, since the electronic selection rules are group-theoretically determined, the calculation of transition moments or oscillator strengths must reflect this. This offers a convenient check on the calculation.

The density matrix calculated from the molecular orbitals is presented in Table IX. The diagonal density matrix elements represent the π-electronic charge densities. The distribution of π-density about the molecule is of course related to the π-dipole moment. The off-diagonal density matrix elements between atomic centers connected by a chemical bond then give the π-bond order between the two centers. Reference to Figure 1 shows that, for instance, atoms 1 and 3 are connected by a bond; therefore, the density matrix element in the first row and third column gives the π-bond order for the 1-3 bond. The off-diagonal elements of the density matrix whose indices are not determined by atoms forming a chemical bond do not carry the physical significance of the other elements, but are sometimes referred to as long-range bond orders. The density matrix is, of course, symmetric. As discussed in the previous chapter, the elements of the density matrix will be used to estimate bond stretching force constants which will subsequently be compared with the corresponding anion force constants.

TABLE VIII

MOLECULAR ORBITALS AND ORBITAL ENERGIES
FOR NEUTRAL TCNE

a_g	b_{1u}	b_{2u}	b_{3g}	a_g	b_{1u}	b_{2u}	b_{3g}	a_g	b_{1u}
-14.8067	-13.9816	-13.5927	-13.5753	-10.8724	-2.8500	-0.2994	-0.2748	0.3180	1.5068
0.2823	0.3614	0.3832	-0.3811	0.2880	0.2750	-0.3218	0.3231	0.2955	0.2091
0.2823	-0.3614	0.3821	0.3822	0.2880	-0.2750	-0.3220	-0.3229	0.2955	-0.2091
0.3089	0.3309	0.3223	-0.3226	0.0900	-0.1883	0.3825	-0.3818	-0.3827	-0.3241
0.3089	-0.3309	0.3214	0.3235	0.0900	0.1883	0.3828	0.3815	-0.3827	0.3241
0.3871	0.1407	-0.0000	0.0000	-0.5638	-0.5271	-0.0000	0.0000	0.1798	0.4499
0.3871	-0.1407	-0.0000	-0.0000	-0.5638	0.5271	-0.0000	-0.0000	0.1798	-0.4499
0.3089	0.3309	-0.3223	0.3226	0.0900	-0.1883	-0.3825	0.3818	-0.3828	-0.3241
0.3089	-0.3309	-0.3214	-0.3235	0.0900	0.1883	-0.3828	-0.3815	-0.3828	0.3241
0.2823	0.3614	-0.3832	0.3811	0.3880	0.2750	0.3218	-0.3231	0.2955	0.2091
0.2823	-0.3821	-0.3822	0.2880	-0.2750	0.3220	0.3220	0.3229	0.2995	-0.2091

TABLE IX

DENSITY MATRIX FOR NEUTRAL TCNE*

	1	2	3	4	5	6	7	8	9	10
1	0.5853	0.03828	0.4791	-0.0066	-0.0023	-0.1040	-0.0137	-0.0063	0.0012	0.0313
2	0.0328	0.5853	-0.0066	0.4791	-0.1040	-0.0023	-0.0063	-0.0137	0.0313	0.0012
3	0.4791	-0.0066	0.4209	-0.0067	0.1154	0.0223	0.0050	-0.0052	-0.0137	-0.0063
4	-0.0066	0.4791	-0.0067	0.4209	0.0223	0.1154	-0.0052	0.0050	-0.0063	-0.0137
5	-0.0023	-0.1040	0.1154	0.0223	0.4875	0.4479	0.1154	0.0223	-0.0023	-0.1040
6	-0.1040	-0.0023	0.0223	0.1154	0.4479	0.4875	0.0223	0.1154	-0.1040	-0.0023
7	-0.0137	-0.0063	0.0050	-0.0052	0.1154	0.0223	0.4209	-0.0067	0.4791	-0.0066
8	-0.0063	-0.0137	-0.0052	0.0050	0.0223	0.1154	-0.0067	0.4209	-0.0066	0.4791
9	0.0012	0.0313	-0.0137	-0.0063	-0.0023	-0.1040	0.4791	-0.0066	0.5853	0.0328
10	0.0313	0.0012	-0.0063	-0.0137	-0.1040	-0.0023	-0.0066	0.4791	0.0328	0.5853

*Note all elements should be multiplied by two.

In order to obtain a reasonably good wave function for neutral TCNE, it was found necessary to employ a lower resonance integral value for the C-C double bond than would be obtained using the exponential form fit to the value of -2.39 eV at 1.39 A. The actual values used in the calculation were: β_{CN} = -3.6 eV, $\beta_{C=C}$ = -2.43 eV and β_{C-C}=-1.79 eV. These were the values used in obtaining the molecular orbitals in Table VIII. It should be pointed out that only the C=C resonance integral was changed to fit experimentally observed quantities.

The electron affinity of the TCNE molecule is of interest since TCNE forms many charge-transfer complexes and is one of the strongest π-acids. The electron affinity can be readily estimated as the negative of the energy of the lowest empty molecular orbital. Since TCNE has been treated as a 10-electron problem, the electron affinity corresponds to the negative of the energy of the sixth molecular orbital. Reference to Table VIII shows this value to be 2.85 eV. Fulton (76) reported an experimental value of 2.37 eV; more recently, however, Lyons and Palmer (77) reported values in the range 2.1-3.5 eV from studies of the photodetachment of an electron from the anion. It appears that the calculation predicts the molecular electron affinity reasonably well.

A similar, but open-shell, calculation (65-67) was performed for the TCNE anion. The molecular orbitals and associated eigenvalues are compiled in Table X. The anion density matrix is tabulated in Table XI. In the radical, hyperfine coupling constants and splitting constants obtained from the electron spin resonance (ESR) spectrum may be used as an auxiliary test of the wave function since the spin densities at the nuclei are related to the π-wave functions. Wasilewski (78) presents

TABLE X

MOLECULAR ORBITALS AND ORBITAL ENERGIES
FOR THE TCNE ANION

a_g	b_{1u}	b_{2u}	b_{3g}	a_g	b_{1u}	b_{3g}	b_{2u}	a_g	b_{1u}
-10.8596	-10.0108	-9.6725	-9.6686	-7.0192	0.0024	3.4687	3.5273	4.1766	6.3311
0.2869	0.3754	0.3915	0.3886	0.2962	0.2725	-0.3129	0.3128	0.2828	0.1866
0.2868	-0.3753	0.3888	-0.3913	0.2962	-0.2725	0.3130	0.3126	0.2828	-0.1866
0.3064	0.3203	0.3137	0.3119	0.0740	-0.2313	0.3898	-0.3903	-0.3882	-0.3065
0.3063	-0.3203	0.3116	-0.3140	0.0740	0.2313	-0.3901	-0.3901	-0.3882	0.3065
0.3844	0.1142	-0.0000	-0.0000	-0.5600	-0.4945	-0.0000	0.0000	0.1966	0.4924
0.3844	-0.1142	0.0000	-0.0000	-0.5600	0.4945	0.0000	-0.0000	0.1966	-0.4924
0.3064	0.3203	-0.3138	-0.3119	0.0740	-0.2313	-0.3898	0.3903	-0.3882	-0.3065
0.3063	-0.3203	-0.3116	0.3140	0.0740	0.2313	0.3901	0.0901	-0.3882	0.3065
0.2866	0.3753	-0.3915	-0.3886	0.2962	0.2725	0.3128	-0.3128	0.2829	0.1866
0.2868	-0.3754	-0.3888	0.3913	0.2962	-0.2725	-0.3130	-0.3126	0.2828	-0.1866

TABLE XI

DENSITY MATRIX FOR THE TCNE ANION*

	1	2	3	4	5	6	7	8	9	10
1	0.6523	-0.0079	0.4425	0.0210	-0.0801	-0.0311	-0.0455	0.0211	0.0437	-0.0082
2	-0.0079	0.6523	0.0210	0.4425	-0.0311	-0.0801	0.0211	-0.0455	-0.0082	0.0437
3	0.4425	0.0210	0.4243	-0.0302	0.1701	-0.0174	0.0330	-0.0298	-0.0455	0.0211
4	0.0210	0.4425	-0.0302	0.4243	-0.0174	0.1701	-0.0298	0.0330	0.0211	-0.0455
5	-0.0801	-0.0311	0.1701	-0.0174	0.5966	0.3261	0.1701	-0.0174	-0.0801	-0.0311
6	-0.0311	-0.0801	-0.0174	0.1701	0.3261	0.5966	-0.0174	0.1701	-0.0311	-0.0801
7	-0.0455	0.0211	0.0330	-0.0298	0.1701	-0.0174	0.4244	-0.0302	0.4425	0.0210
8	0.0211	-0.0455	-0.0298	0.0330	-0.0174	0.1701	-0.0302	0.3243	0.0210	0.4425
9	0.0437	-0.0082	-0.0455	0.0211	-0.0801	-0.0311	0.4425	0.0210	0.6523	-0.0079
10	-0.0082	0.0437	0.0211	-0.0455	-0.0311	-0.0801	0.0210	0.4425	-0.0079	0.6523

*Note all elements should be multiplied by two.

several expressions which have been used to relate the hyperfine coupling constants to spin- and spinless density matrix elements. Incorporating the data in Tables X and XI into the expressions given in (78) leads to calculated coupling constants of 1.72, 2.00, and 2.34. The spacing of the lines is calculated to be 1.39 gauss. Phillips et al. (4) have presented experimental values of 2.00 and 1.56 ± .02 gauss for the doupling constant and splitting respectively. The anion wave function seems, therefore, to yield reasonable predictions about the ESR spectrum.

The SCF wave functions for the neutral molecule and its anion appear to be consistent with the experimental data examined. From the discussion presented in the previous chapter, however, the electronic spectra of the two species are the key quantities. A comparison of the observed spectra with the spectra calculated from the wave functions and semi-empirical parameters discussed earlier should now be undertaken. No reliable data have been reported for the electronic spectrum of the solid TCNE anion. The electronic spectra of solutions of neutral and anionic TCNE in various solvents have been reported, however (79) (80). In performing the calculations an attempt was therefore made to obtain good agreement with the solution spectra of the two species. The bands in the electronic spectra of the solids would be expected to exhibit a shift of ~1500 cm^{-1} (~0.18 eV) to lower frequencies relative to the corresponding bands in the solution spectra. A shift of this nature was observed in the qualitative electronic spectra observed during this study.

The theoretically predicted electronic spectrum of neutral TCNE is presented in Table XII. From the results tabulated in Table XII, it can be seen that the calculated value for the lowest energy

TABLE XII

EXPERIMENTAL AND CALCULATED ELECTRONIC SPECTRUM FOR THE NEUTRAL TCNE MOLECULE

TRANSITION	ENERGY (eV) Obsd.	ENERGY (eV) Calc.	POLARIZATION	OSCILLATOR STRENGTH Calc.
5→6 (B_{1u})[b]	5.05[a]	5.136	Z	0.79
5→7 (B_{2u})		6.971	Y	0.16
4→6 (B_{2u})		7.485	Y	0.94
4→7 (B_{1u})		10.091	Z	0.22
5→8 (B_{3g})		7.024		0.00
3→6 (B_{3g})		7.383		0.00
4→8 (A_g)		10.529		0.00
3→7 (A_g)		10.275		0.00
3→8 (B_{1u})		10.532	Z	0.00

[a] J. Halper, W. D. Closson, and H. B. Gray, Theoret. Chim Acta (Berl.) 4, 174 (1966). Assigned on the basis of calculations performed in this study.

[b] Gives the symmetry of the excited state produced by the indicated electron transition.

electronic transition (assigned here as the transition from the fifth molecular orbital to the sixth) corresponds quite well to an experimentally observed band. Halper et al. (79) studied the electronic spectra of several cyanoethylene derivatives in the region below 6.57 eV. The studies were carried out using methanol and ethanol as solvents. All of these derivatives exhibited only one band in this region that was assigned to an allowed $\pi \rightarrow \pi^*$ transition. This observation is also in agreement with the calculated spectrum given in Table XII.

The relevant data for the calculated and observed electronic spectra of the TCNE anion are presented in Table XIII. Itoh (80) and Webster et al. (52) have published data regarding the electronic spectra of the anion in methyltetrahydrofuran and acetonitrile respectively. Both sets of data show a considerable amount of vibronic fine structure on the bands. The calculated value of 2.956 eV for the lowest-energy electronic transition agress quite well with the value of 2.93 eV extracted from Itoh's (80) study. Webster et al. (52) list absorption maxima at 2.85 and 2.92 eV. The bands observed in the two experimental spectra have been assigned (on the basis of the calculation reported here) to the transition of the radical electron from the sixth molecular orbital to the seventh.

An important observation emerging from the calculated anion electronic spectrum is the prediction of an excited electronic state at a relatively low energy (3.33 eV relative to the ground state energy). The existence of two fairly low-energy excited states of different polarizations is a necessary condition, although not sufficient, for the observation of vibronic effects in both the b_{1u} and b_{2u} modes. For instance, parity arguments used in Equation (3.6) in the preceding

TABLE XIII

EXPERIMENTAL AND CALCULATED ELECTRONIC SPECTRUM FOR THE TCNE ANION

TRANSITION	ENERGY (eV) Obsd.	Calc.	POLARIZATION	OSCILLATOR STRENGTH Calc.
5→6 (A_g)[b]		6.045	Z	0.98
4→6 (B_{3g})		8.722	Y	0.63
3→6 (B_{2u})		8.696		0.00
6→7 (B_{3g})	2.930[a]	2.956	Y	0.74
6→8 (B_{2u})		2.753		0.00
6→9 (A_g)		3.328	Z	0.49
6→10 (B_{1u})		5.334		0.00

[a] Michiya Itoh, J. Am. Chem. Soc., 92, 886 (1970). Assigned on the basis of calculations performed in this study.

[b] Gives the symmetry of the excited state produced by the indicated electron transition.

chapter indicate that the $^2B_{3g}$ state at 2.96 eV may mix with the ground electronic state during normal vibrations of b_{2u} symmetry. Similarly a ^2A_g state predicted to lie 3.33 eV above the ground state may mix with the ground state during b_{1u} vibrations. This result seems to be in complete accord with the experimental observation of intensity effects in both the b_{1u} and b_{2u} normal modes.

At this point, it appears that the wave functions calculated for both the neutral and anion molecules can be used to compute quantities that are reasonably consistent with the experimental data with which they were compared. The problem now becomes one of utilizing the theoretical quantities and semi-empirical parameters to compute the vibronic contributions of the π-electrons to the total infrared intensities of modes ν_{11} and ν_{15} in the neutral and anion molecules.

Estimation of Vibronic Interaction Effects

Several calculations must be performed to ascertain the relative importance of vibronic phenomena in the infrared spectra of TCNE and its anion. Only the b_{1u} and b_{2u} C-C single bond stretching modes are to be explicitly considered in the two systems. The gross differences that exist between the infrared spectra of the two systems have been attributed to these modes (10). Furthermore, the perturbation model discussed in the previous chapter is capable of treating stretching modes only.

The calculation of dipole moments at the appropriate molecular configurations is straightforward once the cartesian displacement coordinates of the nuclei are known. The perturbation calculation of the contributions of the π-electrons to the infrared transition moments

is not quite so straightforward. Equation (3.32) is to be employed to determine the perturbation integrals that result when the closed-shell ground electronic state wave function is perturbed by modes ν_{11} and ν_{15}. Analogously, Equation (3.45) will be utilized to assess the perturbations produced by the corresponding modes in the anion. These perturbation integrals along with the observed vibrational frequencies, and the calculated electronic transition energies and moments can then be used in Equation (3.6) in the preceding chapter to calculate the $\vec{M}_{go,gi}$.

The results of the calculation of the perturbation integrals for the neutral molecule that arise during ν_{11} are presented in Table XIV. It should be pointed out, that the values listed in Table XIV give the perturbation matrix element per unit displacement of Q_{11}. All perturbation matrix elements presented in subsequent tables represent values per unit displacement of the appropriate normal coordinate. For purposes of comparison, the table lists the perturbation integrals calculated with and without consideration of the CI among the excited states. The results of the similar calculation performed to compute the perturbation matrix elements when the perturbation is due to ν_{15} of the neutral molecule are presented in Table XV. The corresponding calculations performed for the TCNE anion are given in Table XVI (b_{1u} perturbation) and Table XVII (b_{2u}perturbation).

Analysis of the results given in Tables XIV-XVII bear out the vibronic selection rules presented by Jones (14). For instance; in the neutral molecule, only $^1B_{1u}$-type states and $^1B_{2u}$-type states should be allowed to mix with the ground (^1A_g) electronic state during b_{1u} and b_{2u} vibrations respectively. Similarly, in the anion, only ^2A_g and $^2B_{3g}$ states should mix with the ground state ($^2B_{1u}$) during the b_{1u} and b_{2u}

TABLE XIV

PERTURBATION INTEGRALS FOR THE ν_{11} MODE IN THE NEUTRAL MOLECULE

i[a]	k	SYMMETRY OF EXCITED SINGLET STATE	$\langle \bar{\psi}_g \lvert \frac{\partial H}{\partial Q_{11}} \rvert \bar{\psi}_{i\to k} \rangle$[b] With CI	Without CI
5	6	B_{1u}	-0.1894	-0.1976
5	7	B_{2u}	0.0000	0.0000
4	6	B_{2u}	0.0000	0.0000
4	7	B_{1u}	0.1616	0.1076
5	8	B_{3g}	0.0000	0.0000
3	6	B_{3g}	0.0000	0.0000
4	8	A_g	0.0000	0.0000
3	7	A_g	0.0000	0.0000
3	8	B_{1u}	0.0132	0.1076

[a]The electronic transition occurs from the i^{th} occupied molecular orbital to the k^{th} virtual orbital.

[b]The actual integral units are eV amu $^{-\frac{1}{2}}$A^{-1}; the values listed are for a unit displacement of Q_{11}.

TABLE XV

PERTURBATION INTEGRALS FOR THE ν_{15} MODE IN THE NEUTRAL MOLECULE

i	k	SYMMETRY OF EXCITED SINGLET STATE	$\langle \bar{\Psi}_g \lvert \frac{\partial H}{\partial Q_{15}} \rvert \bar{\Psi}_{i\to k} \rangle$ With CI	Without CI
5	6	B_{1u}	0.0000	0.0000
5	7	B_{2u}	1.9508	1.5190
4	6	B_{2u}	-0.7024	-1.4112
4	7	B_{1u}	0.0000	0.0000
5	8	B_{3g}	-0.0002	-0.0005
3	6	B_{3g}	-0.0001	0.0020
4	8	A_g	0.0000	0.0000
3	7	A_g	0.0000	0.0000
3	8	B_{1u}	0.0000	0.0000

TABLE XVI

PERTURBATION INTEGRALS FOR THE ν_{11} MODE IN THE ANION

i	k	SYMMETRY OF EXCITED DOUBLET STATE	$\langle {}^2\bar{\psi}_g \lvert \frac{\partial H}{\partial Q_{11}} \rvert {}^2\bar{\psi}_{i\to k} \rangle$ With CI	Without CI
5	6	A_g	-0.2486	-0.2322
4	6	B_{3g}	0.0000	0.0000
3	6	B_{2u}	0.0000	0.0000
6	7	B_{3g}	0.0000	0.0000
6	8	B_{2u}	0.0000	0.0000
6	9	A_g	-0.2599	-0.2747
6	10	B_{1u}	0.0000	0.0000

TABLE XVII

PERTURBATION INTEGRALS FOR THE ν_{15} MODE IN THE ANION

i	k	SYMMETRY OF EXCITED DOUBLET STATE	$\langle {}^2\bar{\psi}_g \lvert \frac{\partial H}{\partial Q_{15}} \rvert {}^2\bar{\psi}_{i\to k} \rangle$ With CI	Without CI
5	6	A_g	0.0000	0.0000
4	6	B_{3g}	0.9595	0.9839
3	6	B_{2u}	0.0004	0.0034
6	7	B_{3g}	0.6244	0.5851
6	8	B_{2u}	0.0000	-0.0002
6	9	A_g	0.0000	0.0000
6	10	B_{1u}	0.0000	0.0000

modes respectively. The calculations all support these selection rules as may be seen from the tables.

All of the quantities required to evaluate the $\vec{M}_{go,gi}$ have now been determined. Substitution of the appropriate quantities into Equation (3.6) of the preceding chapter yields the contribution of the π-electrons to the infrared transition moment of the i^{th} normal mode. A summary of the results of the Herzberg-Teller (15) perturbation calculations is presented in Table XVIII. Also listed in Table XVIII are the contributions to the infrared moments that were deduced from the dipole moment derivatives. Two notable aspects of the data presented in Table XVIII are: 1) that the π-contributions to the transition moments calculated from the dipole moment derivative method are consistently greater in magnitude than the corresponding quantities computed from the perturbation calculation, and 2) the results computed for ν_{15} in the neutral molecule even disagree with respect to their algebraic signs. Some explanation of this result should be sought.

Pople and Segal (83) have indicated that ZDO calculations involving changes in molecular bond lengths are unsatisfactory since the errors introduced by the ZDO approximation are sharp functions of the internuclear distances. This begins to cast some doubt on the results obtained from the distortion calculation. This problem does not arise with the perturbation calculation since all quantities are evaluated at the equilibrium nuclear configurations of the neutral and anion molecules. Also, in the preliminary perturbation calculations which were performed without any consideration of CI among the excited states, a sign opposite to that presented in Table XVIII was obtained for the π-contribution to the intensity of the ν_{15} mode of the nuclear molecule.

TABLE XVIII

CALCULATED VIBRONIC TRANSITION MOMENTS
DUE TO THE π-ELECTRONS

MODE CONSIDERED	DPM[a] (esu cm)	HT[b] (esu cm)	POLARIZATION
ν_{11}, Neutral	-9.5505×10^{-20}	-3.6826×10^{-20}	Z
ν_{15}, Neutral	-3.3468×10^{-20}	2.3898×10^{-20}	Y
ν_{11}, Anion	-5.0391×10^{-19}	-1.4044×10^{-19}	Z
ν_{15}, Anion	8.2432×10^{-19}	2.0079×10^{-19}	Y

[a] From dipole moment derivatives.

[b] From Herzberg-Teller perturbation calculations.

The perturbation calculation allows for the mixing of a certain amount of excited state character into the distorted ground state electronic wave function whereas the self-consistent wave function calculated at a distorted configuration allows for no such mixing due to Brillouin's theorem (69). Furthermore, experience with the dipole moment calculation shows that it is quite sensitive to small changes in the bond lengths. This is due, no doubt, to the exponential form assumed for the bond resonance integrals. Several calculations were carried out assuming the σ-framework to be polarized, with the core charges adjusted accordingly; this also led to large changes in the dipole moments. The perturbation integrals, on the other hand, varied much less rapidly. On the basis of the arguments presented above, it is felt that the data obtained from the perturbation calculation offer the better estimates

of the π-contributions to the various transition moments. All ensuing discussions will, therefore, be based on the data obtained using the perturbation techniques.

In order to obtain estimates of experimental infrared intensities observed in the anion it is necessary to compare the magnitudes and directions of the π-moments in the anion with the framework contributions. The total anion infrared intensity is proportional to the square of the vector sum of the π-electron transition moment, $\vec{M}_{go,gi}$, with the framework moment. It now becomes necessary to estimate the framework moment that developes during a normal mode distortion. It is assumed that the major differences that exist between the neutral molecule and the anion are primarily due to the differences in their π-systems. The framework contributions to the total intensities of corresponding neutral and anion modes are, therefore, assumed to be equal.

Moore et al. (10) reported an experimental value of 1140 Darks for the b_{2u} stretch, ν_{15}, of the neutral molecule. This intensity value leads to a value of the total transition moment of $\pm 1.11 \times 10^{-19}$ esu cm. The algebraic sign of the transition is indeterminate on the basis of the experimental datum. Comparison of this experimental value with the calculated π-electron contribution (2.3898×10^{-20} esu cm), as determined from the perturbation calculation, indicates the framework moment to be the primary source of the infrared intensity. The magnitude of the framework moment will therefore be taken as being roughly the same as the total moment. Reference to Table XVIII shows that the π-moment for the anion is approximately the same as the framework moment. Before anything can be stated about the intensity of ν_{15} in the anion, however, the algebraic sign of the framework moment must be ascertained.

Del Re (81) has reported a method for the calculation of dipole moments that is useful for saturated systems. Kier (82) calculated the total dipole moment of unsaturated systems by treating them as a π-system superimposed on a σ-framework. Kier (81) calculated the π-moment by the standard Hückel method (70) and the σ-moment by Del Re's method (81). The total dipole moment was then obtained as the vector sum of the two moments. The results obtained by this technique were shown to be in generally good agreement with experimental values. Since an "experimental" magnitude is available for the framework contribution to ν_{15}, then all that is required of the Del Re (81) technique is a prediction of the algebraic sign of the framework moment.

No attempt was made to adjust the semi-empirical parameters presented by Del Re (81). The calculated value of the framework contribution was smaller than might be expected (6.67×10^{-20} esu cm) on the basis of the earlier argument concerning the relative magnitudes of the total experimental moment and the calculated π-contribution, but the important aspect of the calculation is the prediction that the framework contribution for a unit displacement of ν_{15} is directed along the negative y-axis. This information coupled with the magnitude of the framework moment completely characterizes the framework contribution to the intensity of ν_{15} in the neutral molecule.

Now, by an earlier assumption, the framework contributions for the ν_{15} mode of the neutral and anion molecules are taken to be equal. Reference to Table XVIII shows that the calculated π-moment is of the same order of magnitude as the framework moment but is directed along the positive y-axis. The vector sum of the two moments will therefore cancel one another. This result would be expected to lead to a smaller

total transition moment for the ν_{15} anion mode relative to the total infrared transition moment in the neutral molecule; hence an intensity washout would be expected for the ν_{15} anion mode.

It is realized that no quantitative statement regarding the intensity effects can, or should, be made. The foregoing discussion is simply intended to illustrate that the theoretical method employed does predict framework and π-moments in the anion of the same orders of magnitude and opposite signs - a necessary condition for intensity loss. How effectively these moments do, in fact, cancel one another has not been determined theoretically.

Unfortunately, an experimental intensity measurement has not been reported for the ν_{11} mode of the neutral molecule. The magnitude of the framework contribution cannot, therefore, be extracted as was done for the case of the ν_{15} mode. It is possible to calculate the algebraic sign expected for the framework contribution using the technique discussed above. An evaluation of the sign of the framework moment indicates that it is directed along the positive z-axis. This is to be compared with the signs of the π-moment that were calculated for the neutral and anion molecules (see Table XVIII). Once again the π-contribution to the anion infrared transition moment is roughly an order of magnitude greater than that determined for the neutral molecule. This is the same situation encountered in discussing the b_{2u} neutral and anion stretching modes and it is conceivable that the same arguments would apply. The implication is that for the ν_{11} mode in the anion, the π-moment is once again predicted to be of approximately the same magnitude as the framework moment but directed in the opposite direction. Intensity "washout" in the anion is certainly not guaranteed, but at

least there is some evidence to qualitatively predict an intensity decrease in the anion.

The calculations of intensity effects in the ν_{11} and ν_{15} modes that result upon anion formation, although admittedly qualitative, are very suggestive. In both cases considered, the calculations predicted framework and π-moments of opposite algebraic sign and indicated that these moments are comparable in their magnitudes. It is felt that on the basis of these calculations coupled with the experimental data a strong case has been built regarding the importance of vibronic phenomena in the TCNE anion.

Thus, the new experimental data and theoretical calculations tend to support the argument that vibronic interaction effects play a significant role in the spectrum of the TCNE anion in particular, and, quite possibly, other conjugated anion systems in general. The occurrence of the electronic transition energies in the denominators of the Herzberg-Teller (15) expansion coefficients would tempt one to draw this conclusion. Other conditions must, of course, be met also, such as the existence of excited electronic states with appropriate symmetries to mix with the ground state during normal vibrations. Further studies of conjugated radicals are in order before any definite statement can be made about the general nature of vibronic phenomena in these systems. The arguments given above indicated that the transfer of an electron to TCNE results in a complete, or very nearly so, reduction of the infrared activity of the b_{1u} and b_{2u} modes. It is reasonable, then to expect that a partial electron transfer to the TCNE molecule should lead to an intermediate intensity loss for these modes. This intermediate loss of intensity has, in fact, been observed in the weak charge-transfer

complex formed between hexamethylbenzene (HMB) and TCNE (10). What was estimated as a ~5% electron transfer from HMB to TCNE produced a 25% decrease in the intensity of the b_{2u} single-bond stretching mode. Since the de-intensification of the b_{2u} mode is dependent upon the degree to which electron transfer to TCNE has taken place, then the intensity effects observed in the anion must be governed by vibronic interactions involving the radical electron.

Another point of interest regarding the HMB complexes is the intensity effects observed for the HMB. The methyl deformation mode of HMB at 1380 cm^{-1} undergoes an intensity enhancement as a result of the HMB donor action. A similar effect has been observed for the corresponding methyl deformation modes of pentamethylbenzene and durene (10). Furthermore, the enhancement of the intensities of the methyl deformation modes of HMB, rentamethylbenzene, and durene appears to be a function of the electron affinity of the acceptor compounds with which they form charge-transfer complexes.

Moszynska (84) also studied the HMB·TCNE complexes. In this study, it was noted that the intensities of HMB modes of different symmetry species were differently influenced. In particular in-plane e_{1u} modes underwent intensity enhancements, as was mentioned earlier, whereas the a_u modes appeared to be unaffected. This is similar to the situation encountered in the studies of the TCNE anion. The existence of this symmetry effect indicates a vibronic mechanism is operative since the presence or absence of vibronic phenomena is determined on a group theoretical basis.

Theoretical Estimates of Force Constant Shifts

In Chapter I of this report, several bond order-force constant relationships were discussed. Particular emphasis was focused on Gordy's expression (39) and also on a formula due to Coulson and Longuet-Higgins (44). It was pointed out that, although Gordy's formulation (39) worked well in many cases, it was more intuitive than rigorous. The expression reported by Coulson and Longuet-Higgins, on the other hand, is rigorous within the framework of the Hückel theory, but is only applicable to systems containing not more than one hetero-atom. It was this state of affairs that led to the development of Equation (3.56). The derivation presented retains the spirit of the arguments used in the earlier relationship developed in (44) but is not restricted to a particular molecular form. Bratoz and Besnainou (74) inspired the derivation presented in this study. The expression in (74) was developed to predict environmental effects on the C=O stretching frequencies in a series of variously substituted carbonyl compounds. Their expression is somewhat simpler than that derived in this study since they were not concerned with any triple bonds.

Some values must be chosen for K_s, K_d, and K_t before the neutral and anion density matrices given in Tables IX and XI can be used to estimate neutral and anionic stretching force constants and, hence, the changes that occur upon anion formation. Wilson, Decius and Cross (54) present a range of values for K_s, K_d and K_t; the values used in the calculations performed in this study were taken as the average values of the ranges presented for each stretching force constant. The actual

values employed in Equation (3.56) were taken as 5.05, 9.70 and 16.3 md/A for K_s, K_d, and K_t respectively.

Table XIX presents the "observed" force constant changes that result upon anion formation. By "observed", it is meant that these force constant changes are determined as the differences between the sets of force constants that provided the best fits to the observed vibrational frequencies of the neutral and anion molecules. All calculated shifts may be seen to be consistent with the corresponding observed quantities in regard to the directions of the changes. The actual values of the shifts are seen to be less well reproduced. Perhaps a better procedure would have been to fit the values of K_s, K_d and K_t to reproduce the force constants observed for the neutral molecule, and then to use these to determine the anion force constants.

TABLE XIX

OBSERVED AND CALCULATED FORCE CONSTANT CHANGES

	Force Constant (md/A)		Difference	
	Neutral	Anion	Observed	Calculated
$K_{C\equiv N}$	17.04	16.34	-0.70	-0.51
$K_{C=C}$	6.59	4.54	-2.05	-1.45
K_{C-C}	5.32	5.68	+0.36	+0.53

An important observation to be made from Table XIX is that the largest calculated force constant change is experienced by the C-C double bond. This is consistent with the assignment of the intense anion band at ~1370 cm^{-1} to the ν_2 mode, since it is this band that exhibits the largest frequency shift upon formation of the anion.

CHAPTER V

SUMMARY AND CONCLUSIONS

The goal of the present study was to determine the extent that vibronic interaction phenomena influence the vibrational spectrum of the TCNE anion. It is known that the infrared spectrum of the TCNE anion is remarkably different from the infrared spectrum of the neutral molecule. The differences range from the appearance of unexpected bands in the anion to the virtually complete disappearance of expected bands. Both of these effects have been ascribed to vibronic interactions involving the unpaired electron.

Earlier studies have assigned the intense features in the 500-2200 cm^{-1} region of the anion infrared spectrum to the totally symmetric (a_g) bond-stretching modes. It was presumed that these normally forbidden modes became activated by the "electron vibration" mechanism initially suggested by Ferguson. The importance of Raman data for the anion is obvious. Previous attempts to monitor Raman scattering from the anion were thwarted by the intense color of the anion. The experimental problem of preparing TCNE anion samples which were suitable for Raman measurements was, therefore, attacked.

Thin-film samples of the radical anion salts of TCNE were prepared by the co-deposition of neutral TCNE with either sodium or potassium onto substrates chosen to optimize the infrared and Raman spectra. Due to the instability of the samples with respect to oxygen and water,

all sample preparation was done in a vacuum cell. Both crystalline and glassy samples were investigated in an endeavor to understand the doublet character of certain modes.

The Raman data obtained in this study fully support the earlier argument that an "electron vibration" mechanism is operative in the anion. All of the intense infrared bands in the 500-2200 cm^{-1} range were found to have Raman counterparts. The Raman data explained the appearance of unexpected anion bands, but the problem of explaining the disappearance of expected infrared absorptions remained.

The 600-1350 cm^{-1} region of the anion infrared spectrum is barren of any significant absorptions. This is surprising since it is in this range that the b_{1u} and b_{2u} C-C stretching modes absorb quite strongly in the neutral molecule. A theoretical explanation of this observation was sought. Ground state wave functions for both the neutral and anion molecules were obtained using the Pariser-Parr-Pople theory. The suitability of the wave functions was determined by comparing some calculated observables with the experimental values. Once a suitable set of wave functions was obtained, the Herzberg-Teller theory was used to obtain vibronic wave functions which were then used to compute the π-electron contributions to the infrared transition moments for the modes of interest. The π-dipole moments were also used to estimate dipole moment derivatives. Nuclear-centered cartesian displacement coordinates have been obtained for the neutral and anion normal modes which were used to obtain the appropriate distorted configurations.

A comparison of the π-contributions to the infrared transition moments as calculated by the two methods just cited led to the conclusion that the Herzberg-Teller theory probably yields the better results.

The infrared transition moment for a given mode was assumed to be proportional to the square of the vector sum of the π-contribution and the framework contribution. The framework contributions were assumed to be equal for corresponding neutral and anion modes. The magnitude of the framework contribution to the ν_{15} mode was obtained from published intensity data after noting that the experimental transition moment was roughly an order of magnitude greater than the calculated π-contribution. The algebraic sign of the framework moment was determined by the method reported by Del Re. Although no experimental intensity data was available for the ν_{11} mode, the direction of the framework moment was determined.

The calculations predicted that the π-contribution to the total infrared transition moment for the ν_{15} anion mode is of approximately the same magnitude as the framework contribution, and is directed in the opposite direction. The two moments, therefore, tend to cancel one another and an intensity decrease is expected for the ν_{15} anion mode. Similar results were obtained for the ν_{11} anion mode. Thus, the calculations supported the experimental observation of intensity washout for the two anion modes that were explicitly considered.

Raman polarization studies indicated that the previous band assignments for the neutral molecule were in error. The ν_3 mode which was originally assigned to a band at 679 cm^{-1} has been assigned to a polarized feature at 535 cm^{-1}. Normal coordinate calculations also suggest that the bands assigned, in earlier studies, to the b_{1u} and b_{2u} C≡N stretching modes should be interchanged.

The new Raman data for the anion, along with the new band assignments presented for the neutral molecule, have led to a reliable set of

force constants for the two systems. In performing the normal coordinate analysis for the neutral molecule, eight force constants were fit to 15 vibrational frequencies using a modified Valence Force Field. Normal coordinate calculations for the anion were hindered by the disappearance of the b_{1u} and b_{2u} modes. Only the stretching force constants were allowed to adjust in the anion calculation; therefore, three force constants were fit to six observed vibrational frequencies.

A relationship which correlates stretching force constants to elements of the density matrix (obtained from the Pariser-Parr-Pople calculation) was developed. The expression was used to predict force constant variations that occur when the anion is formed. The predicted force constant changes correspond quite well with the changes deduced from the normal coordinate calculations. This correlation was taken as further support of the anion band assignments.

Due to the thin-film character of the anion samples prepared in this study and the availability of several laser excitation frequencies, resonant Raman scattering was observed. It was found that samples which gave virtually identical infrared spectra could differ dramatically in their Raman spectra due to resonance effects in certain modes. The differences in the Raman spectra between two otherwise similar samples are believed to arise from slight stoichiometric variations in the samples.

A SELECTED BIBLIOGRAPHY

(1) T. L. Cairns, R. A. Carboni, D. D. Coffman, V. A. Engelhardt, R. E. Heckert, E. L. Little, E. G. McGreer, B. C. McKusick, W. J. Middleton, R. M. Scribner, C. W. Theobald, and H. E. Winberg, J. Am. Chem. Soc., 80, 2775 (1958).

(2) B. R. Penfold and W. N. Lipscomb, Acta Cryst., 14, 589 (1961).

(3) R. E. Merrifield and W. D. Phillips, J. Am. Chem. Soc., 80, 2778 (1958).

(4) W. D. Phillips, J. C. Rowell and S. I. Weissman, J. Chem. Phys., 33, 626 (1960).

(5) T. Takenaka and S. Hayashi, Bull. Chem. Soc. Jap., 37, 1216 (1964).

(6) F. A. Miller, O. Sala, P. Devlin, J. Overend, E. Lippert, W. Luder, H. Moser, and J. Varchmin, Spectrochim. Acta, 20, 1233 (1964).

(7) B. Moszynska, Acta Phys. Polon., 33, 959 (1968).

(8) A. Rosenberg and J. P. Devlin, Spectrochim. Acta, 21, 1613 (1965).

(9) J. Stanley, D. Smith, B. Latimer and J. P. Devlin, J. Phys. Chem., 70, 2001 (1966).

(10) J. C. Moore, D. Smith, Y. Youhne and J. P. Devlin, J. Phys. Chem., 75, 325 (1971).

(11) G. Herzberg, Infrared and Raman Spectra, (Van Nostrand Reinhold Co., New York, 1945), p. 256.

(12) E. E. Ferguson, J. Chem. Phys., 61, 257 (1964).

(13) G. M. Barrow, J. Chem. Phys., 21, 2008 (1953).

(14) W. D. Jones, J. Mol. Spectrosc., 22, 296 (1967).

(15) G. Herzberg and E. Teller, Z. Physik. Chem., B21, 410 (1933).

(16) D. P. Craig, J. Chem. Soc., 1950, 59.

(17) J. N. Murrel and J. A. Pople, Proc. Phys. Soc. (London), A69, 245 (1956).

(18) A. D. Liehr, Z. Naturforsch., 13a, 311, 429, 596 (1958).

(19) A. D. Liehr, Z. Naturforsch., 16a, 641 (1960).

(20) W. E. Donath, J. Chem. Phys., 41, 626 (1964).

(21) W. E. Donath, J. Chem. Phys., 42, 118 (1964).

(22) J. A. Pople and J. W. Sidman, J. Chem. Phys., 27, 1270 (1957).

(23) A. C. Albrecht, J. Chem. Phys., 33, 156 (1960).

(24) J. Overend, Infrared Spectra and Molecular Structure, M. Davies, Ed. (Elseview Publishing Co., Inc., New York, 1963), Chap. 10.

(25) C. A. Coulson and M. J. Stephen, Proc. Roy. Soc., 53, 272 (1957).

(26) E. E. Ferguson and F. A. Matsen, J. Chem. Phys., 29, 105 (1958).

(27) R. S. Mulliken, J. Am. Chem. Soc., 74, 811 (1952).

(28) E. E. Ferguson and F. A. Matsen, J. Am. Chem. Soc., 82, 3268 (1960).

(29) H. Bruce Friedrich and Willis B. Person, J. Chem. Phys., 44, 2161 (1965).

(30) T. L. Brown, J. Chem. Phys., 43, 2780 (1965).

(31) W. D. Jones and W. T. Simpson, J. Chem. Phys., 32, 1747 (1960).

(32) W. D. Jones, J. Mol. Spectros., 10, 131 (1963).

(33) Gary C. Graham and Walter D. Jones, J. Mol. Spectros., 22, 296 (1967).

(34) R. G. Parr, Quantum Theory of Molecular Electronic Structure, (W. A. Benjamin, Inc., New York, 1963), Chap. 3.

(35) R. Pariser and R. G. Parr, J. Chem. Phys., 21, 241 (1953).

(36) Robin M. Hochstrasser, Molecular Aspects of Symmetry, (W. A. Benjamin, Inc., New York, 1966), Chap. 8.

(37) B. R. Penfold and W. N. Lipscomb, Acta Cryst., 14, 589 (1961).

(38) C. A. Coulson, Proc. Roy. Soc., A169, 413 (1939).

(39) W. Gordy, J. Chem. Phys., 14, 305 (1946).

(40) C. A. Coulson and H. C. Longuet-Higgins, Proc. Roy. Soc., A197, 39 (1947).

(41) C. A. Coulson and M. D. Newton, Molec. Phys., 15, 305 (1968).

(42) C. A. Coulson and H. C. Longuet-Higgins, Phil. Mag., 40, 1172 (1949).

(43) R. M. Badger, J. Chem. Phys., 2, 128 (1934).

(44) C. A. Coulson and H. C. Longuet-Higgins, Proc. Roy. Soc., A193, 447, 456 (1948).

(45) R. M. Gavin, Jr. and Stuart A. Rice, J. Chem. Phys., 55, 2675 (1971).

(46) P. C. Li, J. Paul Devlin and H. A. Pohl, J. Phys. Chem., 76, 1026 (1972).

(47) J. Tang and A. C. Albrecht, Raman Spectroscopy, Theory and Practice, Herman A. Szymanski, Ed. (Plenum Press, New York, 1970), Chap. 2.

(48) Paul A. Dobosh, "A Semi-Empirical Molecular Orbital Theory with Intermediate Neglect of Differential Overlap (INDO) and Its Application to the Calculation of Isotropic Hyperfine Coupling Constants", Ph.D. Thesis, Carnegie Institute of Technology, 1969.

(49) Dolan H. Eargle, Jr., J. Chem. Soc. (B), 1556 (1970).

(50) Philip H. Rieger and George K. Fraenkel, J. Chem. Phys., 2795 (1962).

(51) Don Smith, "A Vibrational Study of Matrix-Isolated Nitrates", Ph.D. Thesis, Oklahoma State University, 1971.

(52) O. W. Webster, W. Mahler and R. E. Benson, J. Am. Chem. Soc., 84, 3678 (1962).

(53) J. Overend and J. R. Scherer, J. Chem. Phys., 32, 1289, 1296, and 1720 (1960).

(54) E. B. Wilson, J. C. Decius and P. C. Cross, Molecular Vibrations, (McGraw-Hill Book Company, Inc., New York, 1955), Chap. 4.

(55) B. L. Crawford, Jr. and W. H. Fletcher, J. Chem. Phys., 19, 141 (1951).

(56) Gerald A. Segal and Michael L. Klein, J. Chem. Phys., 47, 4236 (1967).

(57) Ira W. Levin, J. Chem. Phys., 52, 2783 (1970).

(58) D. C. McKean, R. E. Bruns, W. B. Person and Gerald A. Segal, J. Chem. Phys., 55, 2890 (1971).

(59) Roy E. Bruns and Willis B. Person, J. Chem. Phys., 55, 5401 (1971).

(60) Roy E. Bruns, J. Chem. Phys., 58, 1855 (1973).

(61) J. A. Pople, Trans Faraday Soc., 49, 1375 (1953).

(62) R. Pariser and R. G. Parr, J. Chem. Phys., 21, 466, 767 (1953).

(63) C. C. J. Roothaan, Rev. Mod. Phys., 32, 179 (1960).

(64) C. C. J. Roothaan, Rev. Mod. Phys., 23, 69 (1951).

(65) D. A. Lowitz, J. Chem. Phys., 46, 4698 (1967).

(66) V. A. Kuprievich, Int. J. Quantum Chem., 1, 561 (1967).

(67) R. Zahradnik and P. Carsky, J. Phys. Chem., 74, 1235 (1970).

(68) Michel Roche and H. H. Jaffe, J. Chem. Phys., 60, 1193 (1974).

(69) R. Lefebvre, Modern Quantum Chemistry, O. Sinanoglu, Ed. (Academic Press, New York, 1965).

(70) Frank L. Pilar, Elementary Quantum Chemistry, (McGraw-Hill Book Company, New York, 1968), Chap. 12.

(71) N. Mataga and K. Nishimoto, Z. Phys. Chem., 13, 140 (1957).

(72) Inga Fischer-Hjalmers, J. Mol. Spectros., 39, 321 (1971).

(73) H. C. Longuet-Higgins and J. A. Pople, Proc. Phys. Soc., 68, 591 (1955).

(74) S. Bratoz and S. Besnainou, J. Chem. Phys., 34, 1142 (1960).

(75) J. Hinze and H. H. Jaffe, J. Am. Chem. Soc., 84, 540 (1962).

(76) A. Fulton, Aust. J. Chem., 21, 2847 (1968).

(77) L. E. Lyons and L. D. Palmer, Chem. Phys. Lett., 21, 442 (1973).

(78) J. Wasilewski, Acta Phys. Polon., A38, 349 (1970).

(79) J. Halper, W. D. Closson and H. B. Gray, Theoret. Chim. Acta (Berl.), 4, 174 (1966).

(80) Michiya Itoh, J. Am. Chem. Soc., 92, 886 (1970).

(81) G. Del Re, J. Chem. Soc., 4031 (1958).

(82) L. B. Kier, Tetrahedron Lett., 37, 3273 (1965).

(83) J. A. Pople and G. A. Segal, J. Chem. Phys., 43, 5136 (1965).

(84) B. Moszynska, Bull. Acad. Pol. Sci. Ser. Math. Phys., 17, 99 (1969).

APPENDIX

The molecular orbitals, ψ_i, are determined as linear combinations of atomic orbitals, ϕ_μ. For a 2N-electron system, the ψ_i are given be

$$\psi_i = \sum_{\mu=1}^{2N} C_{\mu i} \phi_\mu \tag{A.1}$$

The Pariser-Parr-Pople scheme invokes the π-electron approximation and employs a semi-empirical approach for the evaluation of the dominant integrals. The π-electron Hamiltonian may be written as

$$H\pi = \sum_{\mu=1}^{2N} H_\mu^{core} + \sum_{\mu<\nu}^{2N} \frac{1}{r_{\mu\nu}} \tag{A.2}$$

The first term in Equation (A.2) represents the kinetic energy of the π-electrons plus the nuclear-π-electron attractions and the electronic interactions between pairs (one σ- and one π-electron). The second term in Equation (A.2) represents the electronic interactions between pairs of π-electrons.

Minimization, with respect to the $C_{\mu i}$, of the total π-electronic energy leads to

$$FC_i = SC_iE_i \tag{A.3}$$

where F is the Hartree-Fock matrix, C is the matrix of the atomic orbital coefficients, S is the matrix of overlap integrals, and E is a diagonal matrix of Hartree-Fock eigenvalues.

The F-matrix is expressed as

$$F = H^{core} + 2J - K \tag{A.4}$$

The density matrix may be defined as

$$P = \sum_{i=1}^{N} C_i C_i^t \tag{A.5}$$

where the C_i are column vectors of the matrix that diagonalizes F. Invoking the ZDO approximation, the elements of J and K are given by

$$J_{\mu\nu} = \delta_{\mu\nu} \sum_{y} \gamma_{\mu y} P_{yy} \tag{A.6}$$

and

$$K_{\mu\nu} = \gamma_{\mu\nu} P_{\mu\nu} \tag{A.7}$$

From Equations (A.3) - (A.7) it can be seen that F must be available before the C_i can be computed and that the C_i must be known before F can be determined. This problem is solved by guessing an initial set of C_i to determine F, diagonalization of F then yields a new set of C_i which is in turn used to compute another F. This process is continued until two successive sets of the C_i are equal to within some previously set limit. A reasonable first guess for the C_i may be obtained by setting $F_{\mu\mu} = -\frac{1}{2}(I_\mu - A_\mu)$ and $F_{\mu\nu} = H_{\mu\nu}^{core}$; this is essentially a Hückel calculation. A discussion of the procedures involved when the ground state is an open-shell system will now be undertaken.

Consider an open-shell system which consists of doubly occupied orbitals from 1 to n_1 and singly occupied orbitals from $n_1 + 1$ to n_2. Suppose further that the open-shell system is derived from a neutral molecule that contained 2N π-electrons. The Hartree-Fock matrix for

this system is given by

$$F^{o} = H^{core} + 2J^{c} - K^{c} + \tfrac{1}{2}(2J^{o} - K^{o})$$

$$- \tfrac{1}{2}P^{o}K^{o}(P^{u} - P^{c}) - \tfrac{1}{2}(P^{u} - P^{c})\, K^{o}P^{o}. \qquad (A.8)$$

where

$$P^{c} = \sum_{i=1}^{n_1} C_i C_i^{t} \qquad (A.9)$$

and

$$P^{o} = \sum_{i=n_1+1}^{n_2} C_i C_i^{t} \qquad (A.10)$$

and

$$P^{u} = \sum_{i=n_2+1}^{N} C_i C_i^{t} \qquad (A.11)$$

J^{c}, J^{o}, K^{c}, and K^{o} may be obtained from P^{c} and P^{o} by using Equations (A.6) and (A.7) respectively.

The expressions required for the CI calculation will now be discussed. Only singly excited configurations will be considered. No derivations of the appropriate expressions will be presented; instead, only a rather concise listing of the CI matrix elements will be presented.

The matrix elements of the singlet CI matrix (65) (67) are written as

$$\langle {}^{1}\bar{\psi}_{i\to k} | H | {}^{1}\bar{\psi}_{i\to k} \rangle - \langle \bar{\psi}_{g} | H | \bar{\psi}_{g} \rangle = E_k - E_i$$

$$- \langle ik|G|ik\rangle + 2\langle ik|G|ki\rangle \qquad (A.12)$$

and

$$< {}^{1}\bar{\psi}_{i\to k}|H|{}^{1}\bar{\psi}_{j\to l}> = 2 <jk|G|1i> - < jk|G|i1 > \qquad (A.13)$$

where

$$< jk|G|1i > = < \psi_j(1)\psi_k(2)|\frac{1}{r_{12}}|\psi_1(1)\psi_i(2) \qquad (A.14)$$

and E_k represents the energy of the k^{th} molecular orbital. Equation (A.12) gives the energy, relative to the ground state energy, of the singlet excited state formed by the promotion of an electron from the i^{th} occupied orbital to the k^{th} virtual orbital. The eigenvalues of the CI matrix give the electronic transition energies with an account of CI. The components of the eigenvectors of the CI matrix yield information regarding the make-up of the total wave functions for the excited states.

The analogous expressions will now be presented for the excited doublet states. The transitions to be considered are: 1) from the i^{th} doubly-occupied molecular orbital to the singly-occupied orbital (N+1), and 2) from N+1 to an empty orbital, k. The results are given as (65) (67) (68)

$$< {}^{2}\bar{\psi}_{i\to N+1}|H|{}^{2}\bar{\psi}_{i\to N+1} > - < {}^{2}\bar{\psi}_{g}|H|{}^{2}\bar{\psi}_{g} >$$

$$= E_{N+1}-E_1 + \tfrac{1}{2} < N+1,N+1|G|N+1,\ N+1 >$$

$$+ \frac{3}{2} < i,N+1|G|N+1,i > - < i,N+1|G|i,N+1 > \qquad (A.15)$$

$$< {}^{2}\bar{\psi}_{N+1\to k}|H|{}^{2}\bar{\psi}_{N+1,k} > - < {}^{2}\bar{\psi}_{g}|H|{}^{2}\bar{\psi}_{g}$$

$$= E_k - E_{N+1} + \tfrac{1}{2} < N+1,\ N+1|G|N+1,\ N+1 >$$

$$+ \frac{3}{2} < N+1,\ k|G|k,N+1 > - < N+1,\ k|G|N+1,k > \qquad (A.16)$$

for the energies of the excited doublet states relative to the ground state. The off-diagonal elements of the doublet CI matrix may be written as

$$< {}^{2}\underline{\bar{\psi}}_{i\to N+1} | H | {}^{2}\underline{\bar{\psi}}_{h\to N+1} > = \frac{3}{2} < h,N+1|G|N+1,i > - < h,N+1|G|i,N+1 > \quad (A.17)$$

and

$$< {}^{2}\underline{\bar{\psi}}_{i\to N+1} | H | {}^{2}\underline{\bar{\psi}}_{N+1\to k} > = < N+1,N+1|G|i\ k > \quad (A.18)$$

and

$$< {}^{2}\underline{\bar{\psi}}_{N+1\to k} | H | {}^{2}\underline{\bar{\psi}}_{N+1\to 1} > = \frac{3}{2} < N+1,k|G|1,N+1 > - < N+1,k|G|N+1,1 > \quad (A.19)$$

VITA

Jerald John Hinkel

Candidate for the Degree of

Doctor of Philosophy

Thesis: A THEORETICAL AND EXPERIMENTAL STUDY OF VIBRONIC INTERACTIONS IN THE RADICAL ANION SALTS OF TETRACYANOETHYLENE

Major Field: Chemistry

Biographical:

Personal Data: Born in Wadena, Iowa, January 5, 1948, the son of Donald and Vera Hinkel.

Education: Graduate from Valley High School, Elgin, Iowa in May, 1966; received the Bachelor of Science degree from Upper Iowa University, Fayette, Iowa, with majors in chemistry and mathematics, in May, 1970; completed requirements for the Doctor of Philosophy degree at Oklahoma State University, July, 1974.

Professional Experience: Student Assistant, Upper Iowa University, Fayette, Iowa, 1967-1970; National Defense Education Act Fellow, Oklahoma State University, 1970-1973; National Science Foundation Research Assistant, Oklahoma State University, 1973-1974; Graduate Teaching Assistant, Oklahoma State University, 1970-1974.

Membership in Honorary and Professional Societies: Member of Phi Lambda Upsilon, Honorary Chemical Society; member of the American Chemical Society.